Kungliga Tekniska Högskolan

Machine Design Advanced Course Part II - MF 2077

Development of a Test Rig for Tribological Evaluation of Sliding Bearings in Saline Water

Master's Programme in Machine Design
Academic year 2

Students

Alves Da Silva Crespo Martins Ricardo
Latestere Florian
Lucero Alexander
Pitke Rohit
Redzovic Numan

Professors

Andersson Kjell
Akepati Bhaskar Reddy

0.1 Abstract

Tidal energy is emerging but faces challenges as saline water is very corrosive and requires specific material and sealing solutions. KTH Royal Institute of Technology in Stockholm, Sweden was interested in revitalizing an unused testing rig to understand the tribological effects of operating sliding tidal bearings in saline water. The development of this test rig included ideation, simulations, CAD modeling, manufacturing with machined components, creation of a DAQ system, and short-term testing. The testing of sliding bearings observed the expected wear phenomena and values for the coefficient of friction. Recommendations are provided to the institution so long-term studies can be conducted using this test rig.

Contents

0.1 Abstract . . . 1

1 Introduction **7**
1.1 Background . . . 7
1.1.1 Tidal Turbine . . . 7
1.2 Problem Statement . . . 8
1.3 Scope and Goals . . . 8
1.4 Requirements . . . 8
1.5 Methodology . . . 9
1.5.1 SWOT Analysis . . . 9
1.5.2 Work Breakdown Structure . . . 11

2 Critical Review of Existing Knowledge **12**
2.1 State of the Art . . . 12
2.1.1 Original Test Rig . . . 12
2.2 Literature Review . . . 15

3 Implementation **17**
3.1 Reuse of subsystems . . . 17
3.2 Concept Generation . . . 18
3.2.1 Design Concept 1 - Underwater load cell . . . 18
3.2.2 Design Concept 2 - Load cell above the water . . . 18
3.2.3 Design Concept 3 - Two Central Load Cells . . . 20
3.3 Concept Evaluation . . . 21
3.3.1 Weighted Matrix Criteria . . . 21
3.3.2 Scored Concepts . . . 22
3.3.3 Weighted Matrix and Chosen Concept . . . 24
3.4 Detailed Design . . . 24
3.4.1 Sliding Bearing and Sleeve concept . . . 25
3.4.2 Shaft . . . 25
3.4.3 Friction Torque Measurement System . . . 37
3.4.4 Sealing system and tank . . . 44
3.4.5 Electronics and DAQ . . . 51

4 Proof Of Concept **56**
4.1 Modifications to Final Design . . . 56
4.2 Manufacturing . . . 57
4.2.1 3D Printed Prototypes . . . 58

4.2.2 Tank . . . 58
4.3 Assembly Instructions . . . 59
4.3.1 Shaft Installment . . . 59
4.3.2 General Assembly . . . 61

5 Setup Process **63**
5.1 Machine Electronics Setup Procedure . . . 63
5.1.1 Connections . . . 63
5.1.2 Turn on the Motor . . . 64
5.1.3 Data Acquisition Software . . . 65
5.1.4 Motor Control . . . 66
5.2 Test Setup Procedure . . . 70

6 Results and Discussion **72**
6.1 Load Cell Verification Tests . . . 72
6.2 Methodology . . . 73
6.3 Results . . . 75
6.3.1 Friction Measurement Results . . . 75
6.3.2 State of the Bearing after the tests . . . 80
6.4 Discussion . . . 81

7 Broader Impacts **83**
7.1 Engineering Ethics . . . 83
7.2 Societal and Global Impact . . . 83
7.3 Environmental Impact . . . 83
7.4 Codes and Standards . . . 84
7.5 Economic factors . . . 84

8 Conclusion **85**

9 Future Work **86**

Bibliography **88**

A Comparison of Shaft Material **90**

B Granta Edupack material property description **91**
B.1 B1 - Resistance to Sea Water . . . 91
B.2 B2 - Stress corrosion cracking . . . 91
B.3 B3 - Galling resistance . . . 92

List of Figures

1.1 Tidal turbine illustration . . . 7
1.2 Work Breakdown Structure . . . 11

2.1 Sliding bearing test rig - Loading system [1]. . . . 13
2.2 Sliding bearing test rig - Friction measurement [1]. . . . 13
2.3 Test rig electrical box [1]. . . . 14

3.1 Design Concept 1 - Friction measurement method [1] . . . 18
3.2 Design Concept 2 - Friction measurement method . . . 19
3.3 Design Concept 2 - Detailed Design . . . 19
3.4 Design Concept 2 - Sensor Assembly . . . 20
3.5 Design Concept 3 - Detailed Design . . . 20
3.6 Weighted Matrix. . . . 24
3.7 Chosen design render. . . . 25
3.8 Metal Sleeve (Left), Polymer Bearing (Right). . . . 25
3.9 Sleeve with Keyway. . . . 26
3.10 Mitee Bite. . . . 27
3.11 Ringfeder Locking Element. . . . 28
3.12 Trantorque Locking Element. . . . 29
3.13 Taper on shaft. . . . 30
3.14 Parameters for Cone type hub shaft connection. . . . 31
3.15 Calculated values for a taper connection[13]. . . . 31
3.16 Taper details on the shaft. . . . 32
3.17 3D View of the shaft. . . . 32
3.18 Final Sleeve Design. . . . 33
3.19 Vesconite Test Bearings. . . . 33
3.20 Section View- Support Housings[1]. . . . 35
3.21 3D View- Support Housings. . . . 35
3.22 Stiffness diagram of the MBS model. . . . 38
3.23 Constraint diagram of the MBS model. . . . 39
3.24 MBS Force Results. . . . 39
3.25 Displacement simulation of one of the friction sensor. . . . 40
3.26 Sensor Accuracy Characteristics . . . 41
3.27 Types of Bearings . . . 43
3.28 Housing Comparison . . . 44
3.29 Test rig Water Tank . . . 45
3.30 Dual Rotary Oil Seal Solution . . . 47
3.31 Dry running sealing solutions in Vacuum or Air Functions [12] . . . 47

3.32 Single Rotary Oil Seal Solution . . . 49
3.33 O-ring lip seal solution . . . 50
3.34 Electronic box - Photo . . . 52
3.35 Electronic box - Graph . . . 52
3.36 Part of the block Diagram of version 3.0 of LabView . . . 53
3.37 Front Panel of version 3.0 of LabView . . . 54

4.1 Adapted final test rig design . . . 56
4.2 Adapted Shaft and sleeve assembly . . . 57
4.3 Maufactured parts . . . 57
4.4 3D Printed Parts . . . 58
4.5 Manufactured Tank . . . 59
4.6 Applying grease to support bearings . . . 60
4.7 Sweep test on installed shaft . . . 61
4.8 Sleeve housing (top) and temporary sensor (bottom) assemblies . . . 61
4.9 Completed assembly of test rig . . . 62

5.1 Connection example . . . 63
5.2 Wire box switches . . . 64
5.3 Emergency stop block . . . 64
5.4 Security key . . . 65
5.5 IndraWorks communications window . . . 66
5.6 IndraWorks startup mode . . . 67
5.7 IndraWorks Warning Window . . . 68
5.8 IndraWorks Command Box Control . . . 69
5.9 Test Setup Procedure . . . 71

6.1 Calibration results of the load cells used to measure the friction torque . . . 72
6.2 Calibration results of the load cell used for measuring the applied radial load. . . . 73
6.3 Reciprocating movement profile of the tests . . . 75
6.4 Force sample of the test condition 1 . . . 76
6.5 Moving maximum and minimum results of the first test . . . 76
6.6 Friction torque estimation from the data . . . 77
6.7 Estimated friction coefficient . . . 77
6.8 Measured load sample. . . . 78
6.9 Measured torque sample. . . . 78
6.10 Estimated radial Load variation along the test, only considering the side load cells. . . 79
6.11 Estimated friction coefficient variation along the test. . . . 80
6.12 Bearing and sleeve after test 1. . . . 80
6.13 Bearing test 2. . . . 81
6.14 List of requirements, their priority and verification. . . . 81

List of Tables

3.1 Support Bearing Housing No. 1 34
3.2 Support Bearing Housing No. 2 34
3.3 Load Cell specifications. 42

Chapter 1

Introduction

The courses MF2076 and MF2077 – Machine Design Advance Course Part 1 and 2, respectively, encompassing lectures, assignments, and a project. This document focuses on reporting the progress of Group 5 for the project "Design of a test rig for tribology evaluation of tidal turbine components". The project task consists of designing a test rig to evaluate the tribological performance of reciprocating sliding bearings by replicating the operating conditions of the bearings in a tidal turbine.

Fig. 1.1: Tidal turbine illustration

1.1 Background

1.1.1 Tidal Turbine

Tidal power plants are underwater energy generators harnessing the motion of the tides or the waves to produce electricity. Due to its nature, it is a renewable source of energy.

Various technologies are used to convert the tidal energy to electricity depending on the environment where the tidal power plant is placed. One of the technologies is tidal turbines which are large turbines placed underwater, located in a stream where tides have a great amplitude.

There are few commercial-sized tidal power plants operating in the world but there is potential to become a bigger green electricity source in the future.

Tidal energy converters are subjected to great technological challenges linked to the environment they are operating. Firstly, saline water is very corrosive and requires specific material and sealing techniques. Secondly, the system is subjected to the motion of the tides and the waves whose frequency and amplitude can vary greatly.

The successful tackling of these challenges is highly dependent on the fact that the tribology study of the components and materials submerged in saline water has not been deeply explored.

Tidal energy converters are a new method to produce electrical energy, and time has not allowed researchers to collect enough data to understand tribological effects in underwater conditions.

Moreover, underwater machine maintenance is expensive and requires much time and specific skills. Having underwater components with excellent reliability and well-studied life-cycle and failure possibilities is vital for the tidal energy industry.

Therefore, a need arises to create a test rig that can simulate the conditions that the underseawater turbine is subjected to and obtain knowledge on how the surrounding environment affects the various components and contacts.

The need is to design a test rig able to evaluate the tribological features of components under water and reproduce with the higest fidelity the working conditions that exist in the turbines of tidal energy converters. The primary component chosen for these kinds of studies is the sliding bearing. For that reason, the test rig should be made to test sliding bearings but also allow for modularity and later fit different components.

The emerging technology of tidal energy converters necessitates a deeper understanding of the tribology of components in saline water. As underwater machine maintenance is costly and time-consuming, reliable components with well-studied life cycles are vital for the tidal energy industry. Thus, the project aims to design a test rig to simulate underwater conditions and evaluate the tribological features of components, focusing initially on sliding bearings with provisions for modularity and testing different components.

1.2 Problem Statement

Design a test rig to evaluate the tribological properties of sliding bearings under seawater conditions. The test rig aims to measure friction between the sliding bearing and the shaft under a controlled environment.

1.3 Scope and Goals

The assignment is to be completed within the Machine Design Advanced courses MF2076 and MF2077 at KTH, utilizing the resources provided in the Machine Design Lab. Additionally, components and manufactured parts can be sourced from external companies if needed. The project is divided into two phases: the first phase involves generating detailed concepts for the test rig from January 2023 to June 2023, while the second phase centers on the manufacturing and assembly of the test rig from September 2023 to December 2023.

The objective of the course is to create a test rig, adhering to the outlined requirements in the following section, for evaluating sliding bearings. This test rig should be functional for both KTH researchers and future students.

1.4 Requirements

When defining the project scope with the researchers and PhD students who are going to use the test rig, the system requirements were defined as follows:

- The system shall replicate the operating conditions of the main shaft bearings of a tidal turbine.
- The test rig shall withstand the testing corrosive environment of seawater.

- The test rig shall offer the possibility to actuate the amplitude of oscillation of 1 Hz.
- The test rig shall fit sliding bearings.
- The test rig shall fit sealing rings.
- The test rig shall apply a variable radial load on the test sample applied at the beginning of the test.
- The test rig shall be able to apply a controllable amplitude (total range) of 90 degrees.
- The test rig shall be able to acquire friction torque data change with time.
- The test rig shall be able to acquire velocity data change with time.
- The test rig shall be able to acquire amplitude change with time.
- The test rig shall be able to acquire frequency change with time.
- The test rig shall be able to acquire radial load change with time.
- The test rig shall use the existing journal-bearing test rig as a basis.
- The test rig shall be able to acquire vibration data of the module being tested.
- The test rig shall be able to acquire the temperature of the casing of the module being tested.
- The system shall be able to measure friction coefficient between 0 and 1 per bearing with a precision of $+/-1\%$.
- The system shall be able to apply a contact pressure of $2MPa$.

1.5 Methodology

To perform this project, several weekly meetings were organized to manage the tasks and objectives. Firstly, there were meetings within the scope of the course with the two responsibilities of the course. Secondly, during the first semester, meetings were organized with the PhD candidate who is going to use the test rig in the future. Thirdly, there were also meetings organized within the team to discuss and distribute the work. In addition to these weekly meetings, there was a need to meet with the researcher responsible for ordering the test rig in order to define requirements and validate the different phases of the project.

The working organization was therefore done around these meetings and weekly objectives were determined. Moreover, as a support to the group organization, some analyses were performed to better understand which methodology to use. The next sections introduce some of them.

1.5.1 SWOT Analysis

The SWOT analysis is used to gain a comprehensive understanding of the group's relation to the task by identifying the group's internal and external factors that enable informed decision-making and strategy development. The internal factors are the project's Strengths and Weaknesses while the external factors are the Opportunities and Threats. If the Strengths and Opportunities can be identified, they can be used as leverage to address the Weaknesses and Threats which will improve the project's performance.

The Internal and External factors that have been identified are presented below:

Strengths:

S1. Subject theory fresh for all the members: In the beginning of the first semester, the members of the project group had just completed the Tribology course which covers many of the concepts that will be discussed giving the group a solid theoretical foundation for the project.

S2. Supporting environment: During the tenure of the project, there will be guidance from experienced teachers to point the members in the right direction while making critical decisions.

S3. No company pressure: Because the project is being developed together with the Department of Engineering Design of KTH, there can be more freedom in the definition of the requirements for the project.

S4. Multicultural Team: The group members come from diverse backgrounds and have different thought processes which will allow them to help each other solve problems with different perspectives.

Weaknesses:

W1. Inexperienced team: Most of the group members have not been in a project like this where the team needs to manufacture a complex product to satisfy stakeholder's needs. This can lead to the project being delayed or details being overlooked.

W2. Aim for too much but accomplish too little: The project is extremely broad; thus, the team can become over-ambitious and try to achieve more than is possible based on knowledge and time. If the project becomes too big it can result in a product that does not deliver what is required and thus not satisfying the stakeholders.

W3. Budget undefined: Since we do not have a clear idea about the budget, we are unable to categorize and prioritize what components we should allot more funds to.

Opportunities:

O1. Low-researched topic: This topic is fairly unresearched, hence it is a particularly good opportunity for the members of the group to contribute to this field of study. Even the smallest bit of contribution can lead to a big breakthrough in this research.

O2. Design for Research: The test rig that will be manufactured is intended to be modular and hence has a vast scope of applications in various fields and is not just restricted to the tidal energy field.

O3. Learn about tribology, machine design and wave/tidal energy converters: This topic allows the group to dig deeper into the field of machine design, but it is also especially important to understand the theory behind tidal and wave energy which can be the future of renewable energy.

Threats:

T1. Not much similar research to build our foundation on: As this topic is new there is not much similar work done thus the group is starting from a blank sheet of paper meaning that the acquisition of knowledge can take more time than expected.

T2. Procurement Delays: As this test rig involves a lot of electronic components like motors, sensors, etc. which have long procurement time, delays in procuring these items can lead to a significant impact on project deadlines.

1.5.2 Work Breakdown Structure

One important management tool to define the work in hand is the Work Breakdown Structure (WBS). A WBS is a hierarchical decomposition of a project into smaller, more manageable components. It organizes the work required to complete a project by breaking it down into deliverables, tasks, and subtasks.

The WBS of the project is composed of 5 major stages: Initiation, Planning, Development, Production, and Closure. These are then broken down into several tasks.

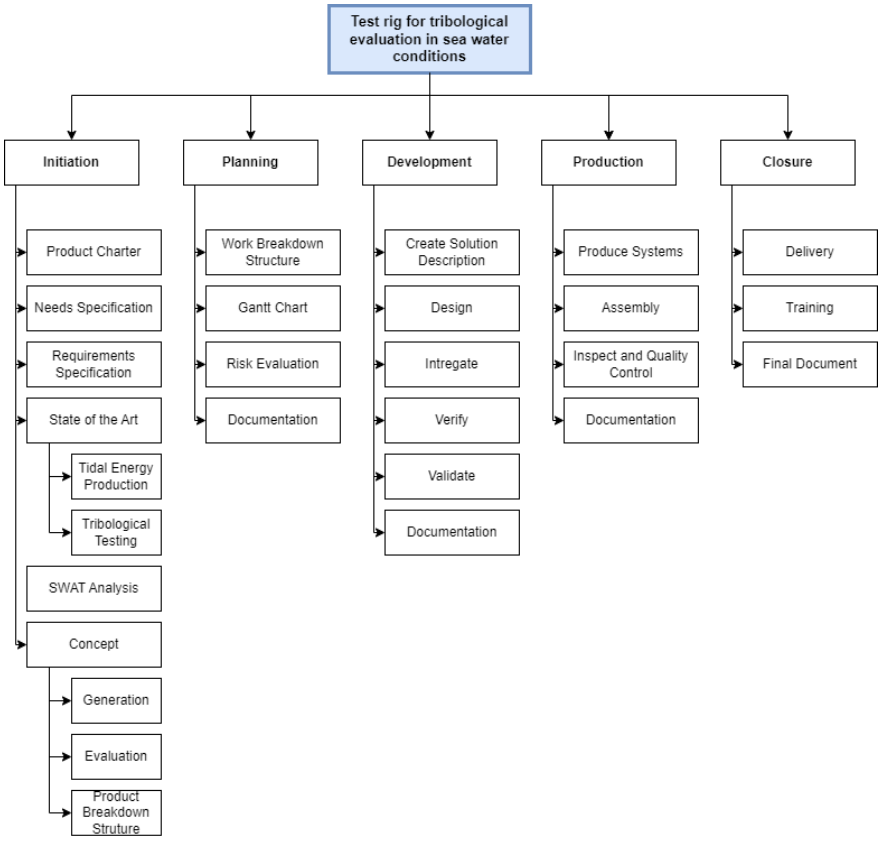

Fig. 1.2: Work Breakdown Structure

For each major step of the WBS, a validation had to be given by the professor to go to the next one. That would ensure that enough work was done before starting working on the next step.

Chapter 2

Critical Review of Existing Knowledge

The test of turbine bearings for tidal energy converters is a very specific topic that at the same time encompasses various areas of research and knowledge. To present this knowledge, two approaches were chosen to be presented in this report: the first, the state of the art, focuses on machines similar to the ones being developed and includes both scientific and non-scientific sources; the second, the literature review, focuses on the scientific research already developed around the study of similar bearings and conditions.

While the first aims to explore concepts that can be used or adapted to the current test rig, the second aims to support the choices of methodologies and conditions of the test that were developed in the end of the development of the test rig.

2.1 State of the Art

2.1.1 Original Test Rig

The Machine Design Department at KTH Royal Institute of Technology has a test rig to measure friction in oil-lubricated sliding bearings. This test rig was developed and manufactured in collaboration with Scania and its purpose was to investigate the tribological performance of sliding bearings in a start-and-stop environment. The rig had not been in operation and conducting science in several years and was no longer required by Scania, thus it provided an opportunity to develop off the existing platform. By modifying the design of the preexisting test rig, new science could be conducted with a reduced development time and cost.

The test rig is built on a steel tubing structure that supports all the major subsystems such as the Power train, Radial load application, friction measurement assembly, and Oil Management system. In Fig. 2.1 the original CAD assembly of the existing machine is displayed.

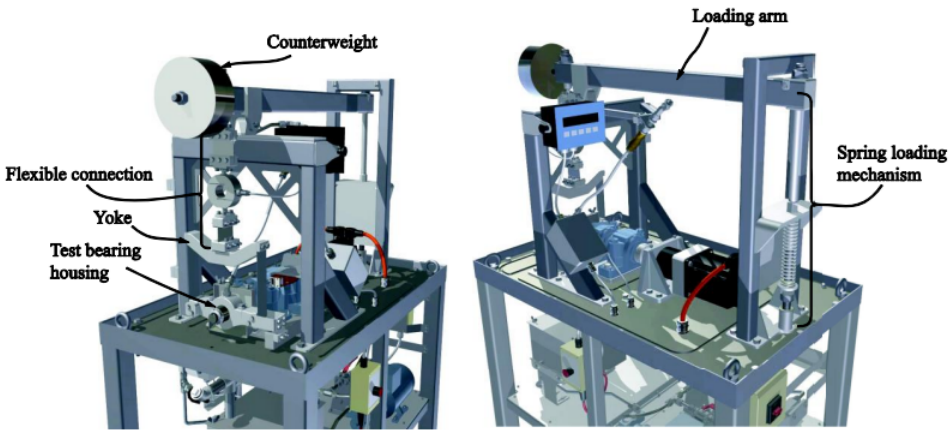

Fig. 2.1: Sliding bearing test rig - Loading system [1].

The friction measurement assembly as shown in Fig. 2.2 is composed of a test-bearing housing where the sliding bearing will be housed. The housing is connected to a yoke using flexible sheets which itself is in turn connected to another flexible connection that connects the whole test-bearing housing assembly to the radial load system. The flexible connections give the housing freedom in all directions and allow for the bearing to self-align to the shaft and to stay straight during operation. The flexible connections not only allow for self-alignment but also ensure that the majority of the fiction torque is transferred to the load cell and not into the sheets of metal.

The friction force is acquired by attaching a bending beam load cell to the right side of the test-bearing housing as seen in Fig. 2.2, and on the left side there are counterweights to balance the system. The friction torque sensor is connected to the housing after the radial load has been applied. When the shaft rotates the bearing will slide against the shaft due to the friction. As a reaction to the friction torque, the test-bearing housing will also start to rotate. The friction force is equal to the force required to stop the test-bearing housing from rotating and as the friction torque sensor is counteracting the friction torque the friction force can be acquired.

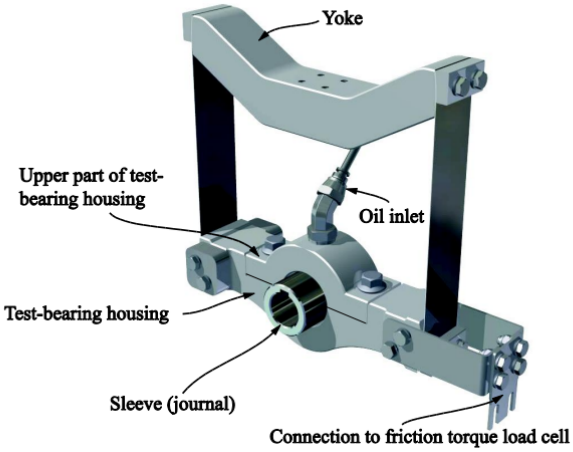

Fig. 2.2: Sliding bearing test rig - Friction measurement [1].

As the conditions of the bearings need to be replicated radial load has to be applied. In this

test rig, the radial load is applied through the loading arm shown in Fig. 2.1. This loading arm is a lever that pulls up the bearing housing when the nut on the top of the spring loading mechanism is tightened, thus applying load on the bottom of the bearing. The radial load is acquired using a load cell rated for 10 kN which is attached to the flexible connections between the yoke and loading arm.

The power train consists of a 16.7 kW Rexroth Indradyn synchronous servomotor (Model Series: MSK060B-0600-NN-M1-UG0-NNNN), which operates at a maximum speed of 6000 rpm. The motor is connected to a Wittenstein LP 090S-MF 1-5 planetary gearbox with a 5:1 reduction that outputs a maximum speed of 1200 rpm to the shaft. Connected to the gearbox, a JAKOB Antriebstechnik Metal Bellow Coupling of KM series is used.

Two support bearings are used:

- Self-aligning ball bearing with tapered bore, SKF 2308 EKTN9, with a SNL 510-608 split housing, a H2308 sleeve, and two TSN 608-S labyrinth seals.
- Spherical roller bearing with re-lubrication features, SKF 22209 EK, with a SNL 509 split housing, a H309 adapter sleeve, and two TSN 509-S seals. Additionally, two locating rings FRB 3.5/85 are installed.

In total, the bearings use 140 g of LGWA-2 grease.

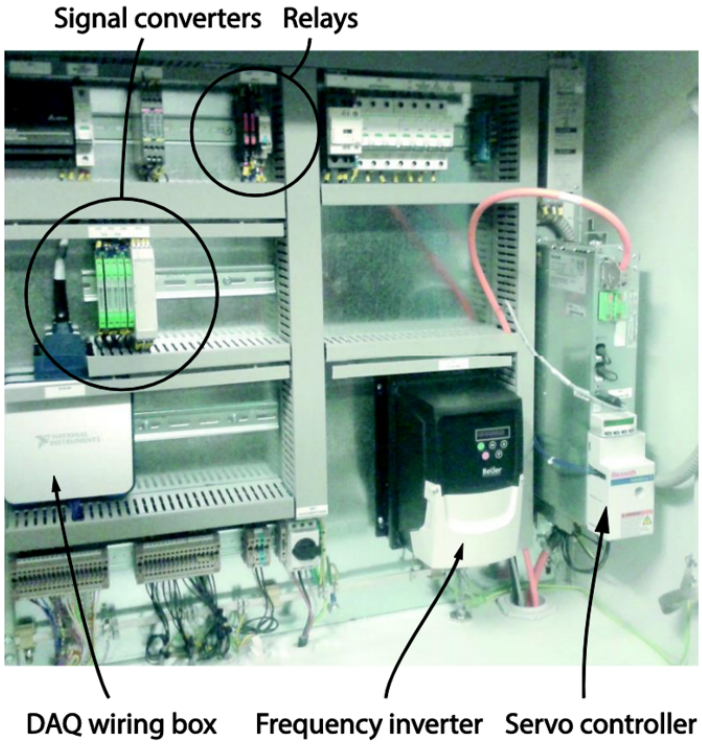

Fig. 2.3: Test rig electrical box [1].

This test rig is also equipped with an electrical box that supplies the rig and DAQ system with power and houses all the electronics as illustrated in Fig. 2.3.

To control the motor, a motor power unit HCS02.1E-W0028-A-03-NNNN is used as well as a motor control unit CSB01.1C-ET-ENS-NNN-NN-S-NN-FW.

Together with the rig a data acquisition system and controlling system was developed. For the control of the motor and oil pump, *IndraWorks* was used while the data acquisition system used *MATLAB*.

2.2 Literature Review

Tidal turbine research is very broad and covers a large amount of research questions. For the purpose of the current project, it is mainly interesting to look into the published articles for other underwater test rigs that could be an inspiration for the design being developed. Therefore, the next paragraphs aim to summarize the features of the underwater test rigs used to test sliding bearings.

The studied rigs have different designs. Firstly, the scale varies, some have small tanks [2] and an easily modified setup. This setup helps to test a lot of different materials and sleeve designs. The bigger rig, [3] and [4], has other external systems to control both the water flow around the tested component and its temperature. The loading system is composed of a screw directly connected to the sliding bearing support that pressurizes the contact, [3] [4]. Overall, two types of setups are installed, the first one as a continuous flow of water around the tested bearing [3],[4] and the second one has non-moving water in a tank, [2]. Moreover, all the concepts found in the literature measure the friction inside the bearing.

Testing conditions and testing setup for other sliding bearing test rigs vary a lot due to different dimensions of the testing subjects and different magnitudes of the radial load that is applied.

In the research paper [5] the researcher's goal was to predict the friction in journal bearings under realistic dynamic working conditions. For their tests, they used a journal bearing with an outer diameter of 76 mm, a width of 34 mm and a nominal clearance of 0.04 mm. The radial load was applied with a hydraulic attenuator with which contact pressures of 40 MPa like modern utility vehicles and a higher specific load of 70 MPa were applied. These loads correspond to a maximum dynamic load of 106 and 180 kN respectively at a frequency of 50 Hz and a shaft speed of 2000 rpm.

On the other hand, the researchers responsible for the paper [6] want to investigate the behavior of journal bearings from hydrodynamic to the mixed lubrication regime. They used the KS Gleitlager journal bearing test rig for a bearing with a diameter of 47.8 mm and a a width of 17.2 mm. Two load cases were investigated with the radial load of 4 kN and 8 kN which generated a contact pressure of 5 and 10 MPa respectively with a constant speed up to 6000 rpm followed by a constant decrease in speed down to zero.

Similarly, another research paper named [7] used the same bearing dimensions as the previous but this time with a much higher load and contact pressures as they were investigating the effects of high pressure on journal bearings in a mixed lubrication regime. Two load cases of 40 kN and 80 kN that gave contact pressures of 50 and 100 MPa, respectively, at 7000 rpm with a run-up and down of 1000 rpm.

These three research papers were tested non submerged journal bearings. Test rigs made for submerged journal bearings have a wide variety of test conditions and setups. In the article [2] a bearing with an inner diameter of $60mm$ was used and three different load cases of 500, 1000 and $2000N$ at speeds of $50 - 1300rpm$ were imposed.

In another rig a journal bearing with a diameter of $100mm$ was employed with an applied average load of 0.2, 0.3 and $0.4MPa$ at $600rpm$ presented in [4].

In the paper [8] a bearing with the diameter of $80mm$ was used rotating at the speed of $0 - 6000rpm$. Radial load in the range of $0 - 6000N$ which corresponded to a contact pressure of $0-1.209MPa$.

Lastly the researchers from the [9] used stainless steel bearings with a load of $4480N$ which gives us a pressure of $0.65MPa$ at $430rpm$.

As it can be seen there are different ways to set up the testing, but the most important thing is to try to replicate the conditions that are going to be simulated. As the testing done in the test rig is supposed to mimic the conditions of journal bearings in tidal turbine applications, the researchers and supervisors for this project were consulted and it could be concluded that a goal of $2.0MPa$ for contact pressure would be sufficient.

Chapter 3

Implementation

This project aimed to reuse and modify the existing test rig. As the machine was already designed for the same purpose to measure the friction force and torque generated between a sliding bearing and shaft, the same general principles could be used for the new case. However, modifications had to be made to accommodate submerged testing in saline water conditions as well as to consider reciprocating motion.

In this chapter, the systems from the previous test rig that were reused in the project are introduced. Secondly, three concepts are described and evaluated. Then one of them is chosen and further developed in the respective detail design.

3.1 Reuse of subsystems

The former test rig had a lot of built-in subsystems that could be of great use for our new design. Reusing subsystems has some advantages, it saves some time that can be allocated to the implementation of new subsystem concepts but it also provides a guarantee that the subsystems are functioning properly as they have been tested and used. Reusing subsystems also impose possible limitations if their use and choice were not properly documented. Considering the advantages and disadvantages of each, three main subsystems were verified and later reused.

The overall structure. The system is placed on a heavy table and the components are attached to a steel plate. This table is sturdy and the steel plate can be very convenient to base our machine on. The structure was therefore reused for our test rig.

The radial load system. As presented in section 2.1.1, the radial load was applied using a lever arm, a bolt, and a spring-loaded mechanism. This subsystem is in good condition and has good performance to apply the load we need. As it is convenient and easily compatible with our system, it was reused for our new test rig.

The power train. As presented in section 2.1.1, motion is transmitted to the sliding bearing using a motor, a coupler, and two support bearings. The motor has performances that fit our application. It is correctly dimensioned to drive a sliding bearing subjected to high load and can perform oscillating motion at 1 Hz and all the software and control units are working properly. The support bearings were examined and it was concluded that they might have been damaged during a previous use of the test rig. Therefore the casing was kept and the bearings were changed. Overall the power train was reused for our new test rig.

3.2 Concept Generation

After consideration of the project requirements and existing structure, the team developed and evaluated three solutions.

3.2.1 Design Concept 1 - Underwater load cell

For the first design concept, the design of the original test rig is kept the same as represented in Fig. 3.1 with the only change being that the original load cell was to be replaced with one that is rated for operation while submerged.

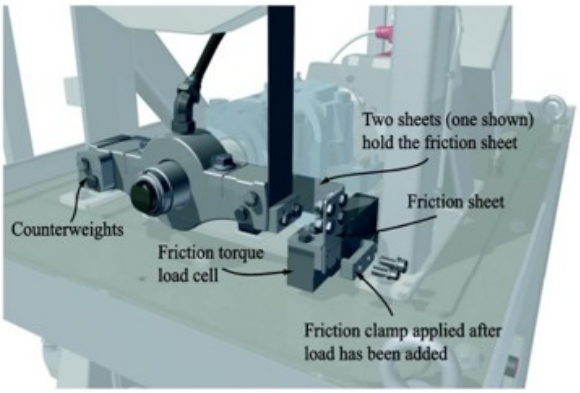

Fig. 3.1: Design Concept 1 - Friction measurement method [1]

When fitting the tank around the test bearing housing the friction sensor must also be submerged if the original design was to be kept due to the close proximity of the friction torque load cell to the housing. The challenge with this design was finding a suitable load cell that satisfies our requirements. There was a limited selection of submersible load cells and the load cells that complied with the requirements were expensive. The effect of saline water on the sensor readings is also uncertain as noise must be minimal. If this design concept was chosen these uncertainties would need to be thoroughly evaluated to verify its feasibility.

3.2.2 Design Concept 2 - Load cell above the water

Very similar to the first design concept, design concept 2 uses the same principle as the original test rig but the sensor is not submerged. Instead the sensor is moved above the waterline as seen in Fig. 3.2.

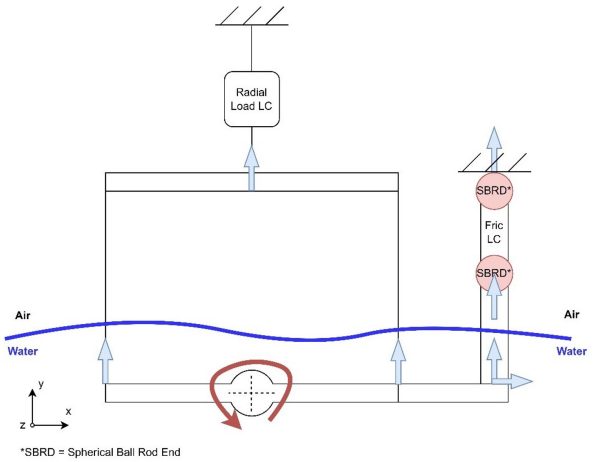

Fig. 3.2: Design Concept 2 - Friction measurement method

For this concept an inline load cell was the sensor of choice, this featured a piezo-electric load cell. The piezo-electric load cell was chosen because of its excellent capabilities to measure dynamic load, this is very important as the design only makes use of one load cell which needs to measure in both directions.

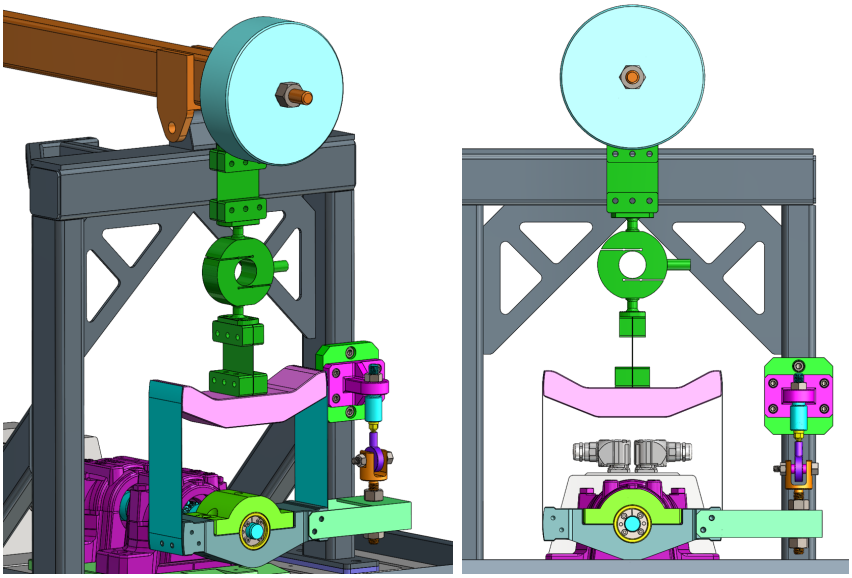

Fig. 3.3: Design Concept 2 - Detailed Design

A major concern with this design concept is the degrees of freedom that either have to be constrained or kept free to ensure that the load cell does not suffer any bending moments. To ensure that this does not happen two spherical ball rod ends were used as illustrated in Fig. 3.4, in this way no bending or transverse loads would affect the load cell.

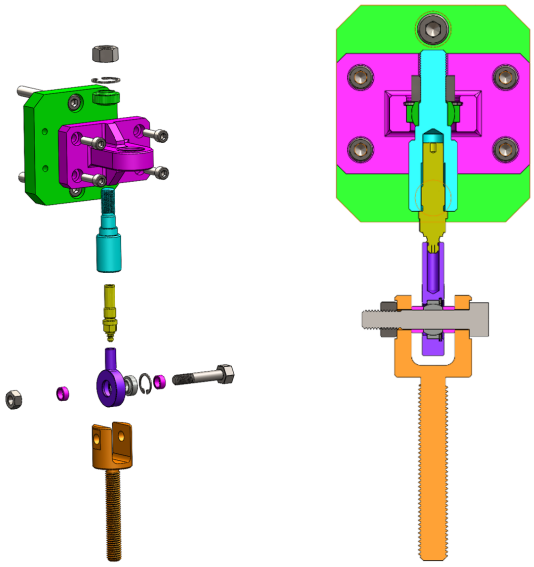

Fig. 3.4: Design Concept 2 - Sensor Assembly

The added freedom also made it possible to make sure that the assembly stayed vertical and aligned with the center of the test bearing on the Z-axis. Furthermore, in order to ensure that no radial load is applied to the friction torque load cell, the friction torque load cell must be mounted after the radial load is applied to the testing bearing.

3.2.3 Design Concept 3 - Two Central Load Cells

The last design concept moved away from the principles of the original test rig and implemented new ideas. For this design concept, a load cell was added to each side of the test-bearing housing attached to the flexible sheets that connect the yoke to the bearing housing as seen in figure 3.5 . This would still allow the test-bearing housing to self-align while also being able to transfer the friction torque to the load cells.

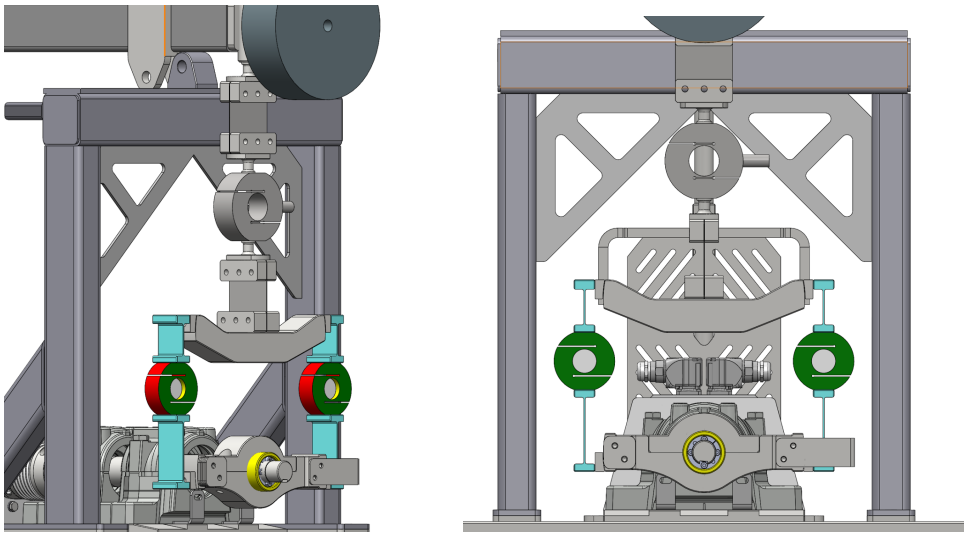

Fig. 3.5: Design Concept 3 - Detailed Design

The friction torque sensors will be reading both the radial load applied to the test bearing as well as the friction torque. By adding the readings of the sensors the radial load could be acquired and by calculating the difference in the peak and trough of both sensors the friction force could be acquired.

The issue with this concept design was finding a suitable load cell. This is because the sensors needed to be able to handle and measure the pre-load of 5000 N while still having the resolution and accuracy to measure the friction force which is significantly smaller in the tenths of a Newton. This concept is also not proven as it is a new idea and it could impose challenges to verify it and make it work as intended.

3.3 Concept Evaluation

The weighted matrix approach was utilized to compare each concept with the stakeholder's needs and specific requirements. This provided a better understanding of the advantages and disadvantages for each concept. By attaching weights of importance to each criterion and scoring each concept based on how well it satisfied the requirements it singled out the concept that best fulfilled the needs for this project. Based on this information an educated decision of what concept to move forward with was made.

3.3.1 Weighted Matrix Criteria

- **Complexity:**

  Describes how difficult the design concept is to implement and how much knowledge there was about it. Complexity can also be defined by the number of components interacting with each other.

- **Ease of Assembly and Disassembly:**

  How easy it could for the researchers to disassemble the testing unit and either prepare it for a new testing sequence using the same test conditions or running a different test and then assembling it back together.

- **Reliability:**

  The reliability criteria defines the robustness of each design concept as the aim of the project was to deliver a test rig that could be used for many cycles without failing.

- **Accuracy:**

  The friction readings needed to be as accurate as possible. This could be affected by the sensor choice and the overall disposition of the design.

- **Costs:**

  The final test rig needs to be cost-efficient. While there was no predefined budget, the cost needed to be reasonable to be approved.

- **Repeatability:**

  The ability to control the testing conditions and ensure that test can be recreated with the same conditions every time.

- **Load Range**:

  Describes how much radial load can be applied to the bearing without compromising the friction torque reading.

- **Modularity:**

  How easy the concept could be altered to accommodate another type of testing subject such as a deep grove ball bearing, seal, or gear pair.

All of these criteria have been graded on importance to the project outcome. This was made on a scale of 1-3 where 3 describes the criteria with the highest importance while 1 describes the criteria with the lowest importance. Although unusual, it was felt that this scale ensures a correct analysis, since the comparison of the values and weights can be easily deconstructed into low, medium, and high priority, without ambiguities.

- **High Importance**

  Reliability and **Accuracy** were the criteria which were assigned a **3** for the highest importance as delivering a test rig that has accurate and scientific measurements and can be used to conduct many test is of the most value to the department and its research.

- **Medium Importance**

  The criteria that were assigned **2** for medium importance are **Complexity** as it was important to deliver a machine to the department that is easy to use and familiar to ensure efficient utilization. **Ease of Assemble and Disassemble** was also assigned a 2 as it allows for the personnel at the department to quickly and easily dismantle the rig to prepare it for a new testing sequence. As well as **Repeatability** was of medium importance as the ability to recreate, control and repeat the testing conditions is crucial for scientific testing. Lastly is high **Load Range** which was assigned medium important as it would allow for varied testing conditions and wider testing range.

- **Low Importance**

  Cost and **Modularity** got assigned the lowest importance as it was believed that the main goal of the project was delivering a test rig that will be of use for the research of the department thus at least guaranteeing that one module or test sample works as intended is of priority.

3.3.2 Scored Concepts

Each concept was evaluated considering the criteria mentioned above. The reasoning behind each classification is given below.

Reasoning's for the scores of Design Concept 1

Complexity (3): For complexity, the first concept scored the highest score as the original test rig is left relatively unchanged only replacing the load cell, thus the concept is already studied and understood.

Ease of Assemble and Disassemble (1): This criterion scored the lowest score as a lot of assembling and disassembling would be done inside of tank which could be very cramped.

Reliability (1): The first design concept scored the lowest score, this time for reliability as it was not really known how the load cell would react to the saline water and how long it would last.

Accuracy (1): Similarly to reliability, the accuracy score is the lowest score as it has uncertainties on how the load cell will react to the saline water as well as how big of an effect the noise

from the water will have on the measurements. The limited selections of load cell could also have made it difficult to find a suitable load cell.

Cost (1): Due to the high price of an underwater load cell the lowest score was given to the first design concept.

Repeatability (2): A medium score was given to the repeatability, this is because the load cell is placed in the water and the added noise from the water can create differences in conditions. Another factor that can create uncertainties is that the load cell is applied after the radial load has been applied.

Load Range (3): For load range this concept was given the highest score as the load cell for radial load measurement and friction measurements are decoupled.

Modularity (3): For the first design concept to be modular the only thing that needs to be altered is the bottom housing. While keeping all the other interfaces the same the only thing that needs to be replaced is this bottom housing.

Reasoning's for the scores of Design Concept 2

Complexity (3): The second design concept still uses the basic principle as the original test rig, thus the test rig is already proven to work.

Ease of Assemble and Disassemble (2): As the load cell was moved above the water line assembling inside of the tank has been kept to a minimum thus a medium score is given.

Reliability (3): The highest score was given for reliability as not many components were left inside the water thus the prolongation of the component life was achieved.

Accuracy (2): A medium score was given for the accuracy as it was believed that some of the reaction forces from the friction moment could be taken up by the sheets that support the test-bearing housing and the link arms in the load cell assembly thus not providing the most accurate results.

Cost (3): As there is a wide variety of load cells to choose from and because only one load cell needs to be acquired this design concept received the highest score for this criterion.

Repeatability (3): For repeatability design concept 2 received the highest score as there is not much that could add unwanted noise to the friction measurement as long as the load cell is n properly attached after radial load is applied.

Load Range (3): For load range, this concept was given the highest score as the load cell for radial load measurement and friction measurements are decoupled.

Modularity (3): For the second design concept to be modular the only thing that needs to be altered is the bottom housing. While keeping all the other interfaces the same the only thing that needs to be replaced is this bottom housing.

Reasoning's for the scores of Design Concept 3

Complexity (2): There was an added complexity due to the fact that this design concept is an unproven idea. The configuration has also been changed compared to the other design concept that could cause unknown issues. Due to these reasons this design concept was given a medium score.

Ease of Assemble and Disassemble (3): As the load cells were attached directly to the housing nothing had to be done inside the tank other than removing the housing from the bearing and the shaft thus, this design concept was given the highest score.

Reliability (3): The highest score was given for reliability as not many components were left submerged in the water thus the prolongation of the component life was achieved.

Accuracy (3): Because the measurements were made very close to the source for this design concept the highest score was given to this design concept for accuracy. Another benefit of this test rig is that the friction moment that would otherwise be lost when taken up by the metal sheets now

will be taken up by the load cell.

Cost (2): A medium score was given to the cost criteria as the load cells that were needed for this application were very specific and could be expensive. New other parts would also have to be manufactured for this to work.

Repeatability (3): For repeatability design concept 2 received the highest score as there is not much that could add unwanted noise to the friction measurement as all the measurements are made with the same load cells.

Load Range (2): The load range was limited for this design concept as the selection of load cells that could be chosen from is limited thus this criterion is given a medium score.

Modularity (3): For the second design concept to be modular the only thing that needs to be altered is the bottom housing. While keeping all the other interfaces the same the only thing that needs to be replaced is this bottom housing.

3.3.3 Weighted Matrix and Chosen Concept

The results of the Weighted matrix are shown in the table 3.6.

Criteria\ Concepts	Complexity	Assembling and Disassembling	Reliability	Accuracy	Cost	Repeatability	Load range	Modularity	Total
Weight	2	2	3	3	1	2	2	1	
1. Underwater	3	1	1	1	1	2	3	3	**57**
2. Side beam above	3	2	3	2	3	3	3	3	**84**
3. 2 load cells	2	3	3	3	2	3	2	3	**83**

Fig. 3.6: Weighted Matrix.

From the table it is possible to verify that the concept that got the highest score is the second concept, with a score of 84 compared to 83 for concept 3 and 57 for concept 1. Although the score is very tight, the concept to move forward with is the second concept with the load cell to the side and above the water.

3.4 Detailed Design

After the concept evaluation process (Section 3.3), the chosen concept has been further refined and some changes were made to accommodate new considerations:

- The piezoelectric sensor was abandoned and replaced by an S beam load cell. The main reason was the price of this type of sensor and its performance with oscillating motion. The sensor requirements and selection are further discussed in subsection 3.4.3.
- The friction measurement system was doubled. This subsystem is now symmetrical around the bearing. This gives the possibility to preload the sensor. As we are working with oscillating motion, if the sensor is not preloaded, it would operate around its zero. This is the least precise zone for the sensor. Preloading the sensor would solve this problem.

This section details the concept chosen which has later been implemented. The next subsections present in detail some aspects of the machine and the design process that led to their design. Fig.3.7 shows a render of the test rig in the final design.

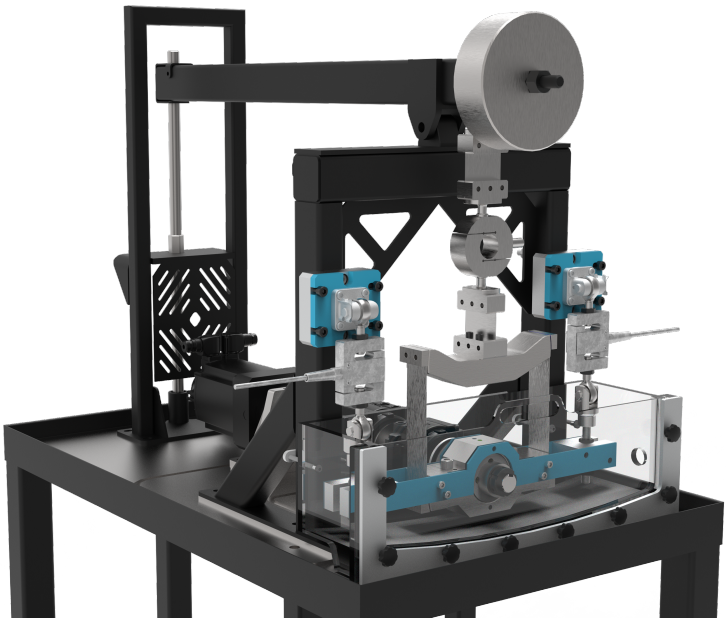

Fig. 3.7: Chosen design render.

3.4.1 Sliding Bearing and Sleeve concept

The sliding/journal bearing comprises a rotating sleeve and a stationary bearing, see Fig. 3.8. Ideally, each component should be composed of two materials to optimize performance. In this instance, the metal sleeve represents the rotating component, while the stationary component is a polymer-based bearing.

The motor transfers oscillatory motion to the shaft through the gearbox and coupling. As a result, it is imperative to attach the rotating sleeve to the turning shaft securely.

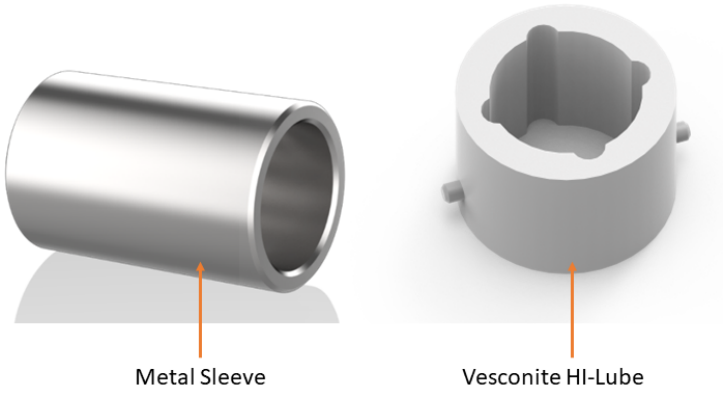

Fig. 3.8: Metal Sleeve (Left), Polymer Bearing (Right).

3.4.2 Shaft

The shaft serves as a crucial component for power transmission from the gearbox to the sleeve. It is connected to the motor and the gearbox via a coupling on the input side, while the output

side is connected to the sleeve. This section details the diverse connection options for attaching the sleeve to the shaft and discusses the support bearings that rigidly uphold the shaft.

Shaft and Sleeve Interface

This section explores different ways of connecting a shaft to a sleeve for transmitting power. The efficient power transfer between these components is crucial. The discussion will focus on different interfaces, their unique features, and how they facilitate power transmission technically.

Keyway Drive

A keyway drive is a power transmission system that uses a key and keyway to connect rotating components, like a shaft and a hub. The key fits into machined slots, preventing relative rotation and ensuring efficient torque transfer, see Fig. 3.9.

The advantages of this system are as follows:

- Easy to assemble and disassemble.
- No axial displacement on locking.
- Easy to manufacture.
- No restriction on workpiece guide length.

The disadvantages of this system are as follows:

- Tighter tolerances are required to maintain a minimum clearance between the key and the sleeve.
- Not suitable for oscillating motions as frequent changes in direction can cause extra wear on the keyway.

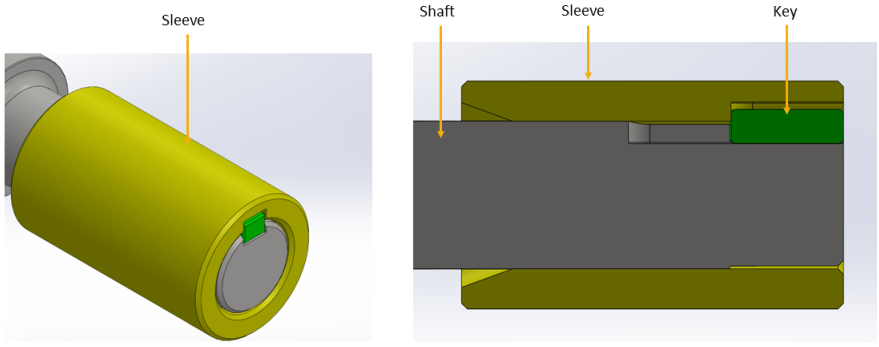

Fig. 3.9: Sleeve with Keyway.

Taper Locking Element

This section highlights various locking elements that utilise a tapered connection instead of a key and keyway mechanism for power transmission.

Mitee Bite

Mitee Bite's ID expansion clamps Fig. 3.10 utilise a taper bolt mechanism to achieve a secure and precise grip on the inner diameter of a workpiece. This involves the application of radial force through the taper bolt, ensuring effective clamping for various machining or assembly applications.

The advantages of this system are as follows:

- Concentric Gripping.
- Ease of assembly and disassembly.
- Negligible axial displacement on locking.
- Easy to source from a supplier.

The disadvantages of this system are as follows:

- Shorter workpiece clamping length maximum 17.5mm.
- An Additional component is required to connect the Mitee bite to the shaft. E.g. Bolted flange connection.
- Unknown saline water compatibility.

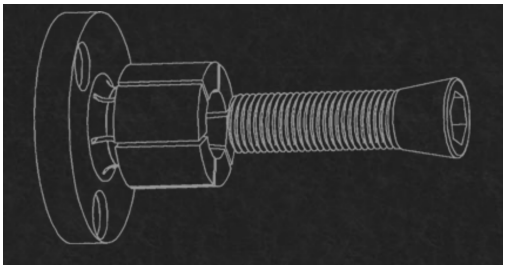

Fig. 3.10: Mitee Bite.

Ringfeder

The Ringfeder locking element [10] comprises two components featuring two opposite tapers. When the bolts are tightened, the locking element undergoes expansion in outer diameter and contraction in inner diameter, effectively clamping both the shaft and the sleeve simultaneously Fig. 3.11.

The advantages of this system are as follows:

- Concentric gripping.
- Minor axial displacement on locking.
- Easy to procure.
- Two locking elements can be used in series to increase the Workpiece guide length.
- Intermediate component can prevent damage to the shaft in case of failure.

The disadvantages of this system are as follows:

- Hard to assemble and disassemble.
- Longer assembly and disassembly time due to extra components (16 Bolts and two locking elements).
- Added complexity with an extra number of components.
- No saline water compatibility.

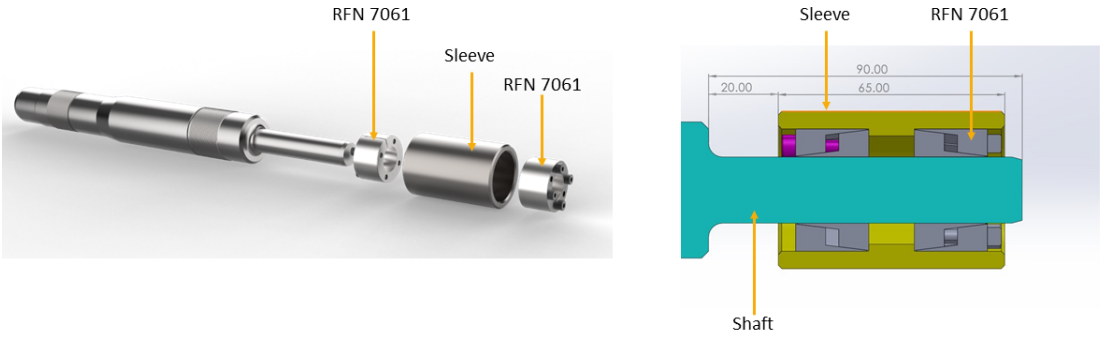

Fig. 3.11: Ringfeder Locking Element.

Trantorque

The Trantorque locking element consists of two components with opposing tapers. A single nut is used to tighten these two tapers against each other. When the nut is tightened, the locking element expands in outer diameter and contracts in inner diameter, securely clamping both the shaft and the sleeve simultaneously Fig.3.12.

The advantages of this system are as follows:

- Concentric gripping.
- Easy to procure.
- Two locking elements can be used in series to increase the workpiece guide length.
- Intermediate components can prevent damage to the shaft in case of failure.

The disadvantages of this system are as follows:

- Unknown saline water performance.
- Unknown axial displacement on locking.
- Limited workpiece clamping length.

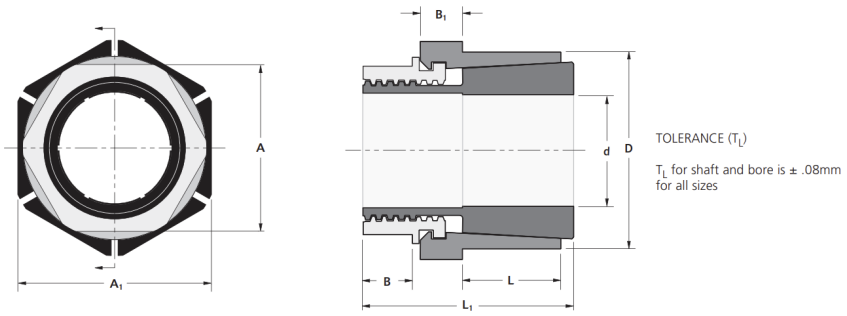

Fig. 3.12: Trantorque Locking Element.

Taper on shaft

The taper-on shaft method involves incorporating an external taper on the shaft and an internal taper on the sleeve. These components are then assembled using a locknut, with the sleeve pushed onto the shaft's taper, creating a friction drive for power transmission. The force generated by the friction between the sleeve and the taper determines the effectiveness of the power transmission. 3.13

The advantages of this system are as follows:

- High concentricity between the sleeve and the shaft.
- Compact assembly, as no intermediate element exists.
- Less dimensional restrictions.
- Easy to manufacture.

The disadvantages of this system are as follows:

- Hard to disassemble.
- Hard to estimate the torque carrying capacity as the coefficient of friction is unknown and can only be approximated.
- Failure can lead to damage to the shaft.

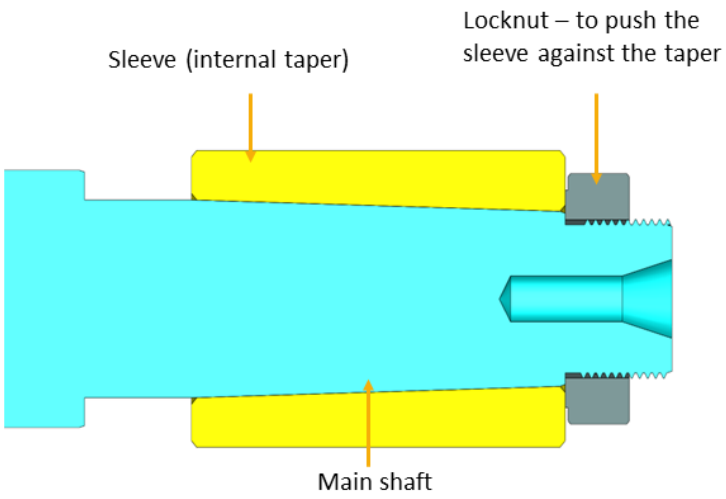

Fig. 3.13: Taper on shaft.

Conclusion

In conclusion, after a thorough comparison of various factors and types of shaft and sleeve interfaces, the Taper of Shaft interface is the optimal choice for the system. This selection offers more control over the material selection of the shaft, coupled with enhanced design and dimensional freedom. Despite posing a challenge in disassembly, this drawback is deemed negligible as the importance is placed more on system performance. Additionally, the Taper on the Shaft interface stands out for its high concentricity, elimination of intermediate components, and ease of manufacturing. Considering all these aspects, it is evident that the Taper on Shaft interface stands as the most advantageous solution for our shaft and sleeve interface.

Details of the Taper

Various machine tapers standards are prevalent across machinery, broadly categorised into 1) Self-locking tapers and 2) Self-releasing tapers. Self-locking tapers, secured in position when properly seated, achieve stability through the wedging action of a small taper angle. In contrast, self-releasing tapers, also known as Steep tapers, are primarily used for alignment purposes.

In this specific application, where the taper must not only ensure a concentric fit but also facilitate power transmission, self-locking tapers are deemed more appropriate. The Morse taper, a standardized form for clamping tools in machine tool holders, is one such self-locking taper. Specifically, the Morse taper 4 (MT4) aligns perfectly with the dimensional constraints of the shaft.

The standard specifications for a Morse taper 4 (MT4) are [11]:

1. $D1 = \varnothing 31.267mm.$
2. $D2 = \varnothing 25.908mm.$
3. $L = 52mm.$

Calculations: The calculations were made using the book [12]. The Fig. 3.14 refers to the different parameters involved in the calculations for the cone type hub shaft connection.

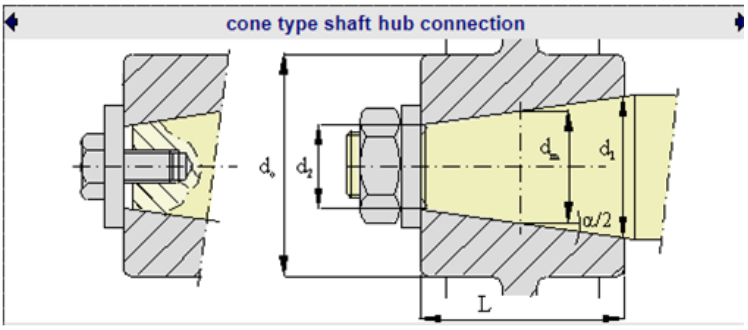

Fig. 3.14: Parameters for Cone type hub shaft connection.

According to the book [12], the shaft-hub connection is self locking when $\mu = tan(\frac{\alpha}{2}) = \frac{d_1 - d_2}{L/2} = C/2$ where, $C = \frac{d_1 - d_2}{L}$. and α = cone angle.

The value of C for the hub-shaft connection to be self locking should be between 0.1 to 0.2. The C value calculated for the current design is 0.1. Hence, it can be concluded that the system will be self-locking. As the friction coefficient is unknown, the friction coefficient μ is considered as 0.05 which is a coefficient of friction for a well lubricated contact. Using the values and the cone type hub shaft connection calculator on Tribology ABC TribABC.

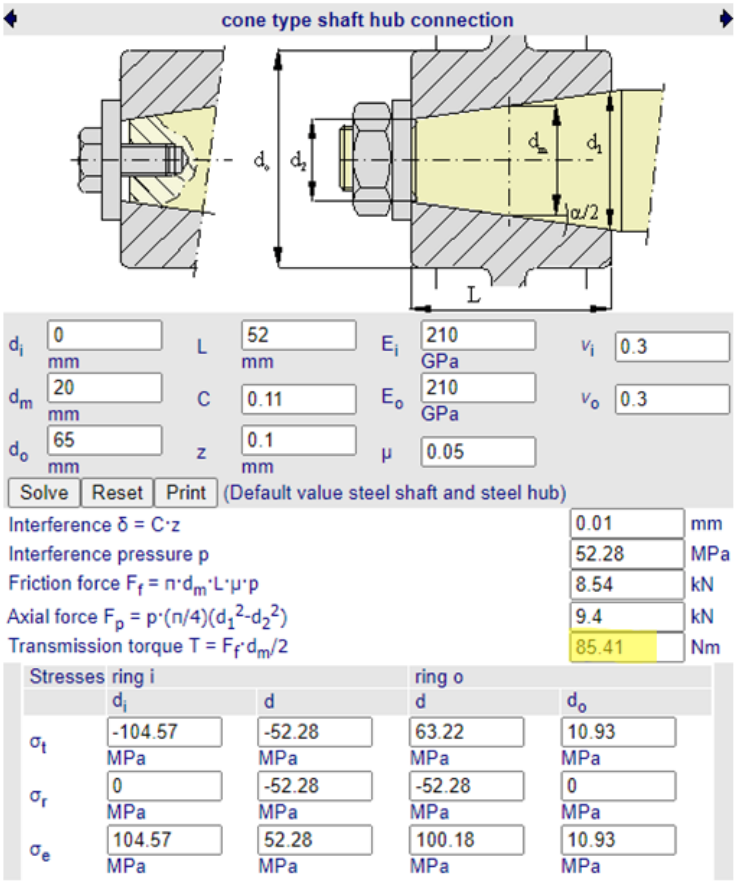

Fig. 3.15: Calculated values for a taper connection[13].

The details of the taper on the shaft are shown in the Fig. 3.16

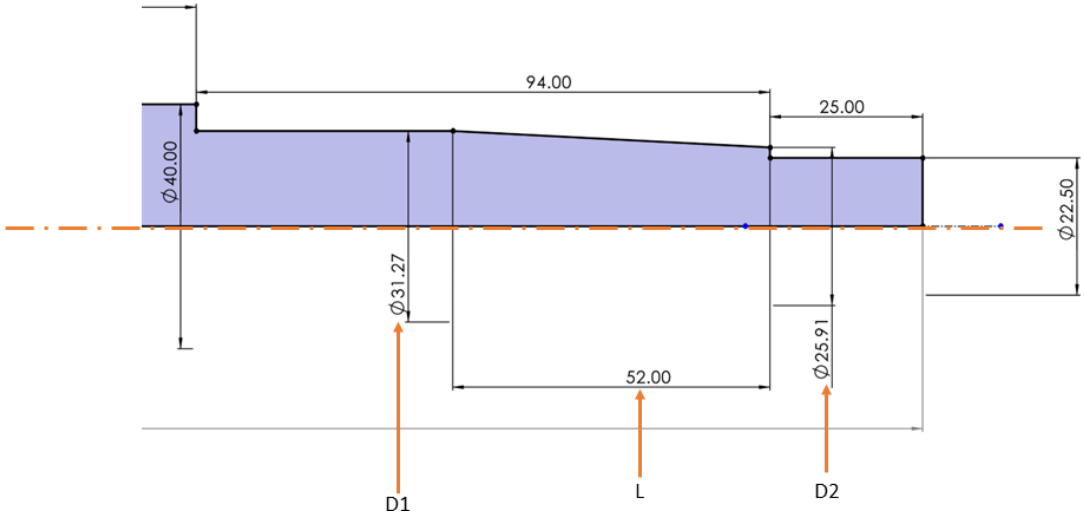

Fig. 3.16: Taper details on the shaft.

From Fig. 3.16, with a maximum transmissible torque of 85.41 Nm and the maximum output torque from the gearbox at 72 Nm, the taper connection, with the MT4 taper, proves to be secure for use as a hub-shaft connection. The transmissible torque capacity exceeds the system's maximum torque, ensuring a safe and reliable application. Furthermore, a keyway is incorporated into the taper as a fail-safe mechanism to mitigate potential damage to the shaft in worst-case scenarios. Fig. 3.17 refers to the final design of the shaft.

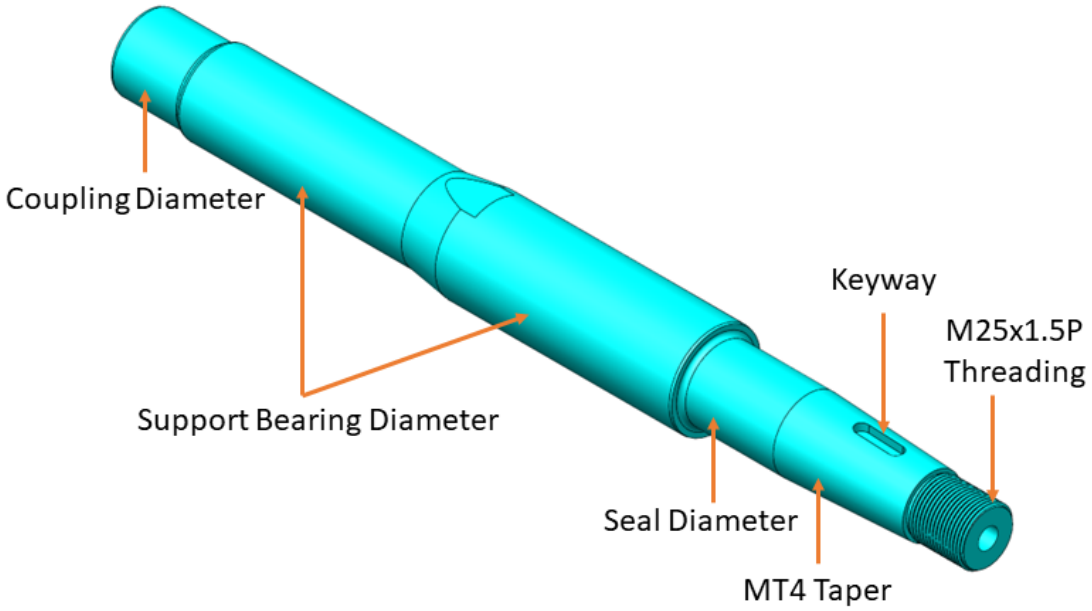

Fig. 3.17: 3D View of the shaft.

Details of the Sleeve

The sleeve was designed to match the specifications of the shaft, incorporating an internal MT4 taper and a keyway. The material composition of the sleeve can be adjusted to accommodate specific material combinations. For the current design, a sleeve manufactured from AISI 316 material was chosen. Refer Fig.3.18 for the details of the final sleeve.

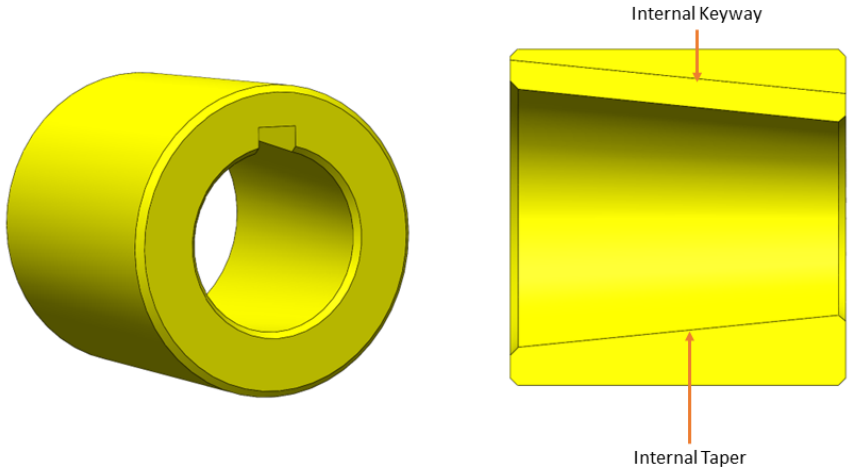

Fig. 3.18: Final Sleeve Design.

Details of the Test bearing

The bearings for this project are sponsored by Vesconite, a company renowned for producing materials tailored specifically for marine environments. Vesconite offers a choice between two distinct materials: 1) Vesconite Hi-Lube and 2) Vesconite Super-Lube. Notably, Vesconite Super-Lube is expected to demonstrate a lower friction coefficient compared to Hi-Lube, although it comes with the trade-off of an anticipated higher wear rate. Refer Fig.3.19.

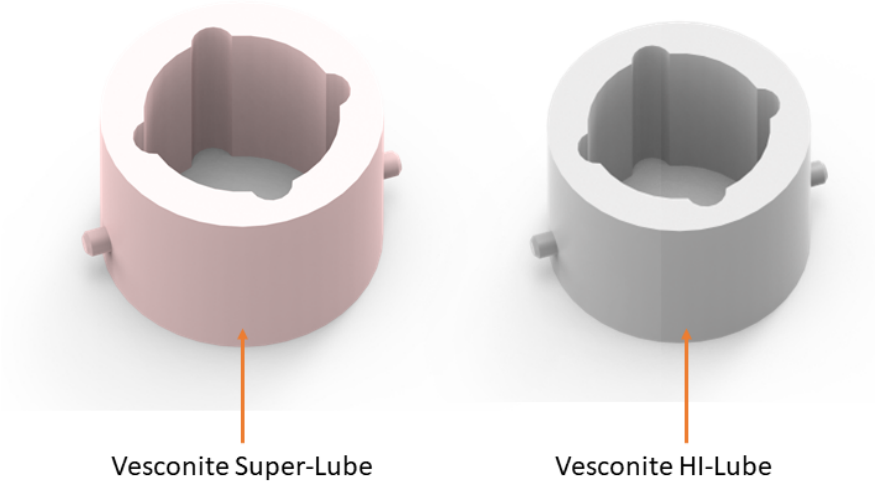

Fig. 3.19: Vesconite Test Bearings.

Support Bearing and Shaft Interface

The shaft is supported by two robust self-aligning bearings capable of accommodating a certain degree of misalignment. The shaft is connected to a gearbox through a flexible coupling; the supporting details for the bearing housings are outlined in this section. Refer Fig.3.20 and Fig.3.21

Support Bearing Housing 1- SKF-SNL 510-608 + 22308 EK + H 2308 + TSN 608 S. The specifications of the parts included are mentioned in the table 3.1

Tab. 3.1: Support Bearing Housing No. 1

Sr. No.	**Model No.**	**Specification Description**
1	SKF_SNL_510-608	Split Housing
2	SKF 2308 EKTN9	Self-aligning Ball Bearing with Tapered Bore
3	H 2308	Sleeve
4	KM8	Locknut
5	TSN 608-S	2 x Labyrinth Seal

Support Bearing Housing 2- SKF-SNL 509 + 22209 EK + H 309 + TSN 509 L. The specifications of the parts included are mentioned in the table 3.2

Tab. 3.2: Support Bearing Housing No. 2

Sr. No.	**Model No.**	**Specification Description**
1	SKF_SNL_509	Split Housing
2	SKF 22209 EK	Self-aligning Roller Bearing with Tapered Bore
3	H 309	Sleeve
4	KM9	Locknut
5	TSN 509 L40	2 x V-ring rubber seals
6	RB 3.5/85	2 x Locating rings

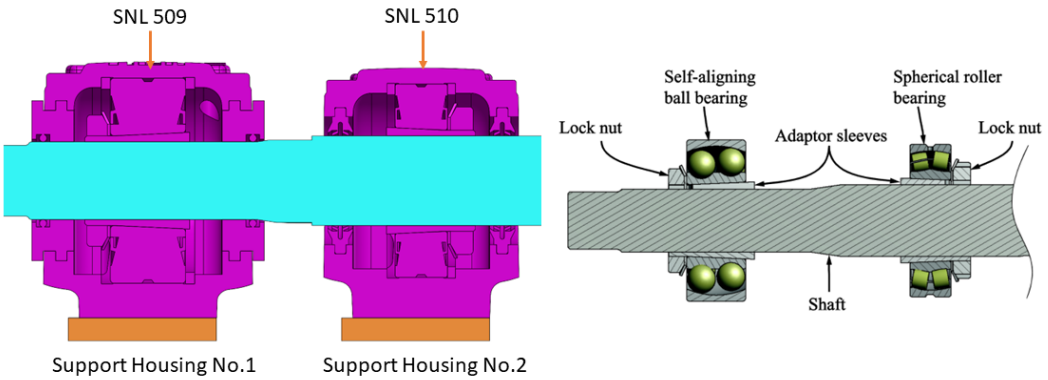

Fig. 3.20: Section View- Support Housings[1].

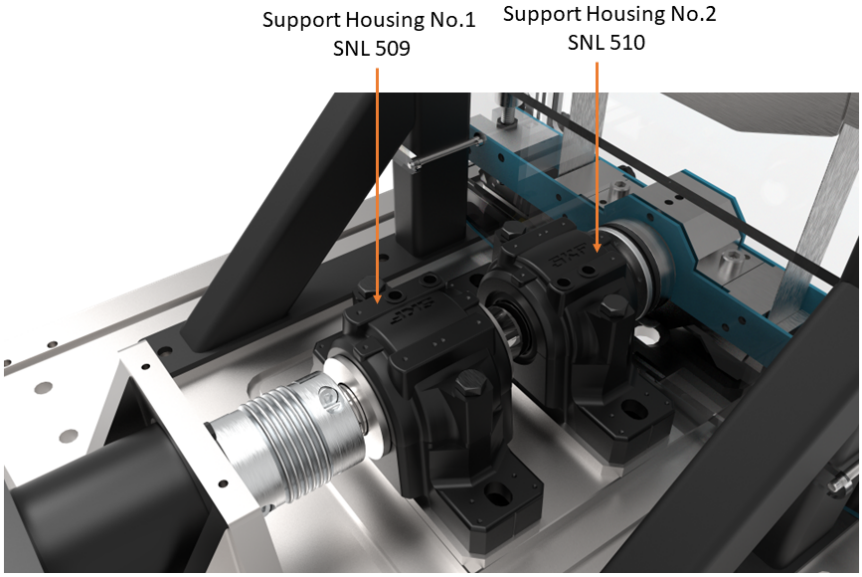

Fig. 3.21: 3D View- Support Housings.

Material selection

The selection of materials for shafts is a crucial decision in engineering design, particularly when considering factors like corrosion resistance in environments such as seawater, mechanical properties, manufacturability, and cost. This section provides a concise overview of various materials, including stainless steels and nickel alloys, comparing their capabilities in resisting seawater corrosion.

Material Requirements
To initiate the process, a definitive list of requirements has been defined as follows:

- The material shall have a hardness in the Rockwell C Scale of (HRC) 55 or equivalent with a depth of at least $0.3mm$ on the surface.
- The material shall be able to be manufactured to have a surface roughness of $Ra = 0.1$ to $0.2\mu m$, $Rz = 1.2\mu m$ for bearing and seal diameters.

- The material must be available in a bar form with a minimum diameter of $50mm$.
- The shaft material should be resistant to seawater for extended periods ($> 3000h = 50$ tests, each with $60h$).
- The shaft has an external Morse Taper 4 (MT4) with a locknut. Hence, the shaft material shall have enough strength and hardness to avoid galling, and a standard KM or YSR locknut will be used to lock the taper in place.

Materials Considered

The alternatives include metals with and without additional treatment (coatings, platings, paint, etc.). Below is a brief description of each of the materials.

Stainless Steel 316L

Stainless steel is a common material used in marine applications especially Stainless steel 316. This material has excellent properties against rust and would satisfy the corrosion requirement, however, this material brings other issues that need to be considered.

The first issue with stainless steel is the strength and hardness of the material. It is softer than regular structural steel, hence creating problems with shaft damage and cold-welding between the seal and the shaft as it needs to be mounted with high force. Thread stripping can also occur due to the softer material and the high force needed for the locking nut, which causes problems for the longevity of the shaft, which is a goal of using stainless steel. Another issue with stainless steel is that its surface cannot be hardened to the same extent as regular steel, in this application, a hardness above 55 HRC is desired while the hardens of stainless steel is limited to 39 HRC. [14]

Stainless Steel AISI 440C with chrome plating

AISI 440C is a Martensitic 400 series stainless steel with the highest carbon content of the 400 stainless steel series. It can be heat-tempered to reach a hardness of 58 to 60 HRC.

This stainless steel can be machined well, with all operations, such as turning, drilling, etc., in the annealed condition. As heat treated, the 440C steel series are complex to machine because of their high hardness. The effect of different heat treatment processes and their subsequent effects on the material properties are provided in A.

The most commonly used chrome plating for this stainless steel is Class 2E due to the long-term service and due to the bore material's high hardness [15].

Nickel-Fe-Cr alloy INCOLOY 945X

The INCOLOY 945X alloy is another material with excellent rust-resistant characteristics suitable for saltwater applications; it is also remarkably similar in strength to regular steel and would be able to handle the test conditions. This material is tough to manufacture and requires specific tools to machine this alloy.

Stainless Steel DUPLEX 2205

Duplex 2205 is a two-phase, ferritic, austenitic stainless steel. It is the most widely used duplex stainless steel grade and is characterized by high yield strength. It demonstrates good fatigue strength, as well as outstanding resistance to stress corrosion cracking, crevice, pitting, erosion, and general corrosion in severe environments. It is generally used in marine environments.

Duplex 2205 is more challenging to machine than the 300 series Austenitic stainless steel. Higher cutting forces are required, and more rapid tool wear is typical.

Steel S275JR

The S275JR grade steel is a readily weldable low-carbon manganese steel with good impact resistance. It is commonly supplied in untreated or normalized conditions. Its machinability is similar to that of mild steel.

Galvanization (Zinc Coating):

Galvanization is often used in the car industry to protect parts from rusting, and it is also used in marine applications but together with an added coat of paint to increase the protection against rust as in this case, it is with high probability submerged underwater. For this test rig, a galvanized steel shaft was considered. Contact was made with SSAB, a provider of Zinc coatings. According to the information provided by the technician at SSAB, steel coated with their Zinc coating Galfan, and subjected to salt spray testing per EN ISO 9227, exhibits surface rust after approximately 500 hours as the coating gradually flakes off during use. Given that our shaft will be submerged, surface rust is expected to manifest in less than 500 hours. Since our tests are anticipated to run for 60 to 100 hours, the coating would, at best, endure for 3-4 tests before necessitating replacement. Consequently, this treatment option was dismissed.

Discussion and Conclusion

Following the compilation of materials under consideration, a comprehensive analysis is undertaken. B presents a tabulated dataset for each material, encompassing parameters like Young's Modulus, Hardness, saltwater resistance, etc., all sourced from the Granta Edupack 2023 R1 database. Qualitative properties of the materials are elucidated in B.

Examining the data in B reveals significant variations among the considered materials in terms of saltwater resistance, galling resistance, stress corrosion cracking, and pricing. Feedback from machining suppliers indicated that, among the listed materials (excluding AISI 316L), only AISI 440 was recognized by the company.

DUPLEX 2205 and INCOLOY 945X were eliminated due to their specificity and cost. S275JR was discarded owing to unknown seawater resistance and low hardness. The chosen material was AISI 440C, hardened through tempering. Despite its high hardness and excellent galling resistance, it exhibits limited durability against saltwater and stress corrosion. However, the application of a chromium plating treatment can enhance its corrosion resistance.

The decision to use AISI 440C with chrome plating is supported by the findings of [16], which highlight the advantages of chromium-plated coatings in marine environments. Nonetheless, challenges such as the evolution of microcracks under mechanical loads pose potential issues in chrome plating, as noted in [16].

Referring to, [15], Stainless Steel 440C, tempered and chrome-plated, can achieve a hardness of $62 - 64$ HRC. Post-grinding and lapping, the surface attains a chrome thickness of $1.3 - 38\mu m$and a surface roughness of Ra $0.091 - 0.183\mu m$. It's noteworthy that a thicker layer of hard chrome coating (approximately $0.4mm$) can yield a finished layer with a thickness of $0.2mm$.

Note: The utilization of a thicker layer of hard chrome coating, around $0.4mm$, can result in a final layer thickness of approximately $0.2mm$.

3.4.3 Friction Torque Measurement System

As stated before, the chosen concept to measure the friction torque of the sliding bearing was concept 2 with one sensor outside of the water.

An initial consideration of piezoelectric sensors was made due to the cyclic load being applied to the measurement system. After discussions with more experienced people, it was concluded that

a piezoelectric sensor is not necessary to fulfill the requirements of load and oscillation. Therefore, the concept of the load cell was rethought, and a strain-gauge load cell was considered.

It needs to be stated that due to the functioning method of the strain gauge load cells, it is desired that the load cells be pre-loaded. The most accurate range of the sensor is in the middle of the range, so measurements around $0N$ should be avoided.

In the end, a similar concept to concept 2 was chosen but instead of only one sensor to the side, it was chosen to use one sensor on each side of the bearing. By taking advantage of the assembly process, it would be possible to pre-load the strain gauge load cells thus using them in the most accurate range.

To ensure that this concept would be suitable to the needs of the project and to also ensure that the theoretical reasoning and assumptions were correct, a Multi-Body Simulation (MBS) was performed. To do it, SimScape Multibody was used.

In order for the multi-body system (MBS) model to represent reality it needs to consider three main aspects: stiffness of the parts, applied loads and degrees of freedom/constraints.

Stiffness of the parts The stiffnesses of the parts were determined in three different ways depending on the nature of the parts: (1) if the parts are simple, the stiffness was calculated internally by the MBS software using the material properties and the geometry; (2) the stiffness was determined using manufacturers datasheets (for instance in the case of the sensor); (3) the stiffness was determined using Finite Element Analysis.

After determining the individual stiffness of each part, if a group of parts was going to be coupled, an equivalent stiffness was calculated, Equation 3.1. This is the case for the friction measurement system, K_M, and the radial load sensor, K_U, Fig. 3.22.

$$\frac{1}{K_M} = \frac{1}{K_{fork}} + \frac{1}{K_{sensor}} + \frac{1}{K_{support}} \tag{3.1}$$

To evaluate the friction measurement system stiffness, the relationship between the load and the deformation needs to be assessed. To do so, a static analysis was performed. Using the module on SolidEdge, a force was applied to the system CAD and then the deformation was measured. Using these two values the system's stiffness can be approximated.

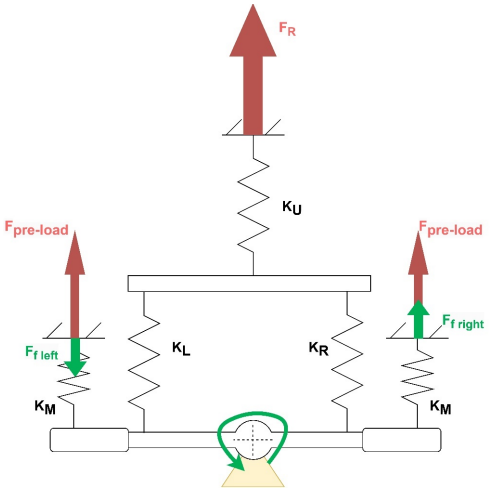

Fig. 3.22: Stiffness diagram of the MBS model.

As the software does not allow for a stiffness value, for instance in N/m, a part with an equivalent stiffness was created. An arbitrary dimension was defined, and Young's Modulus was defined

according to the equivalent stiffness. Poison's ratio was kept at 0.30 since the equivalent parts are not going to be subjected to shear stress and are not going to deform substantially.

All the parts that do not have a stiffness associated in Fig. 3.22 were considered to be infinitely stiff (do not suffer any deformation) due to their geometric nature when compared to the other parts.

Applied Loads Both Friction Load Cells were pre-loaded with 250N, and the load applied on the radial load sensor is 1500 N. In total then, 1500N are being applied to the bearing. A cyclic torque with an amplitude of 9 Nm and frequency of 1 Hz. The torque was obtained by multiplying the radial load by 0.2. From the literature review, a friction coefficient of 0.12 could have been considered. This value is over-dimensioned to 0.20. This friction torque was then multiplied by the internal radius of the bearing.

Applied Constraints The places and joints applied are presented in Fig. 3.23.

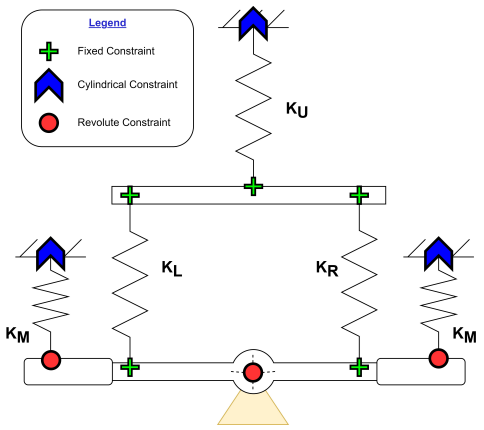

Fig. 3.23: Constraint diagram of the MBS model.

Results By performing the MBS simulation, it was possible to verify that the system could work. The measurements of the friction load cells can theoretically measure the friction torque of the bearing, see Fig. 3.24.

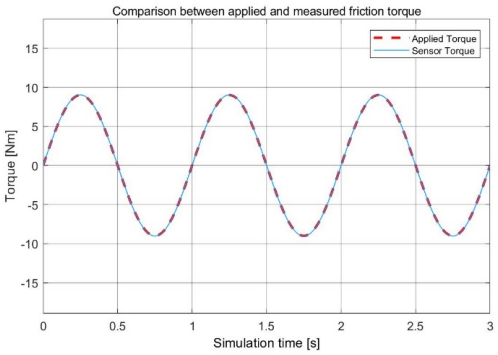

(a) MBS friction torque result comparison between applied torque and measured torque.

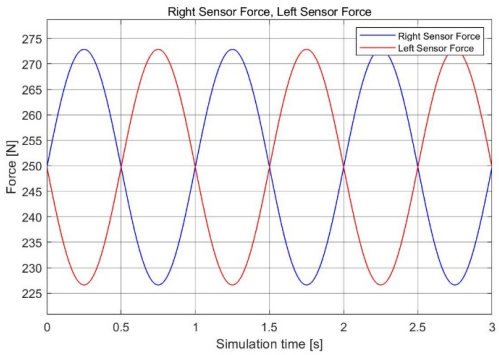

(b) Reading of each one of the friction sensors.

Fig. 3.24: MBS Force Results.

Additionally, the vertical deformation of one of the friction sensors was analyzed, Fig. 3.25 and

verified that it does not exceed 0.02 mm. Knowing this value allows comparisons with possible plays that can exist in the system and also to validate the simulation results.

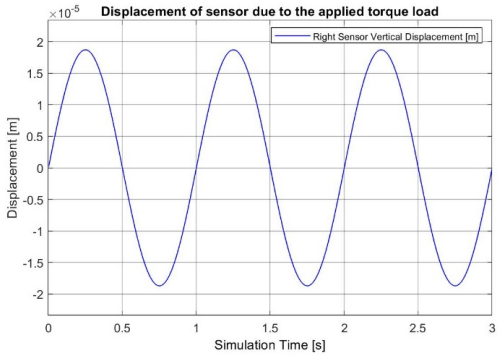

Fig. 3.25: Displacement simulation of one of the friction sensor.

Sensor Selection

Sensor Requirements

The requirements for the friction sensor strain gauge load cell are:

- The sensor shall be able to measure loads in a tensile direction.
- The sensor shall be able to be connected to a TI AD/DA device.
- The maximum measurable load of the sensor shall be able to measure shall be at least $500N$.
- The sensor shall be able to be fitted in the current design.
- The sensor shall have a natural frequency much higher than the frequency of oscillation of the machine ($1Hz$).
- The sensor shall have a specification of the dynamic loading higher than the one expected in the testing rig ($10^6 cycles$).

Among these requirements, there is a desire for the load cell to exhibit high precision when paired with the AD/DA device. To assess the precision of the load cells, various factors can be taken into consideration:

- Non-linearity - the algebraic difference between the output at a specific load and the corresponding point on the straight line drawn between the outputs at minimum load and maximum load, see Fig. 3.26.
- Hysteresis - the algebraic difference between output at a given load descending from the maximum load and output at the same load ascending from the minimum load, see Fig. 3.26.
- Non-repeatability – when a load is repeatedly applied to a load cell, the output of the load cell can vary slightly on each application of the load.
- Creep - change of load cell signal that occurs under load. If a load is continually applied to a load cell, then the output will gradually change over time (creep).

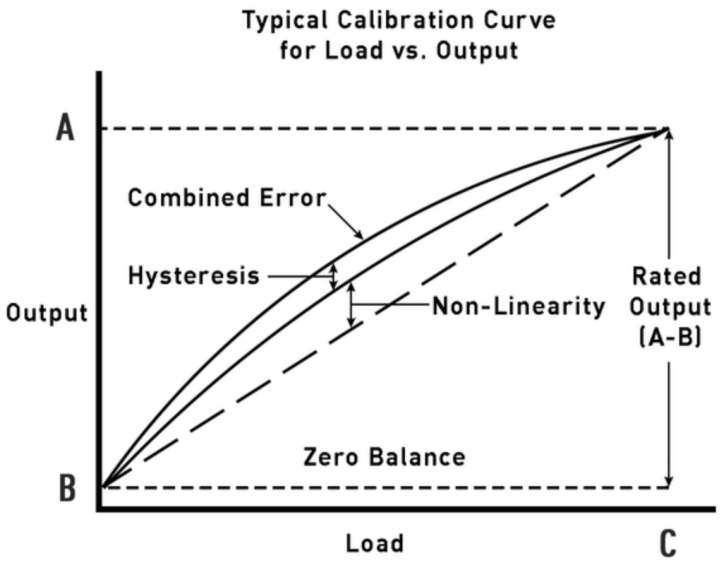

Fig. 3.26: Sensor Accuracy Characteristics

Sensor Model Comparison

Following these requirements, 4 quotes were asked from different manufacturers. The chosen range was 0-500N, and all the sensors are S-type miniature. If the same manufacturer had different options with similar characteristics, the one with the fatigue rating was chosen.

The selected sensors are:

- Interface SSMF-500N
  - Price: 5 050 SEK/pc (VAT incl: NO, Shipping incl: NO).
  - Delivery time: 1-2 weeks (if the product is out of stock 4-6 weeks).
- Applied Measurements DBBE-50kg-003-000
  - Price: 3 525 SEK/pc (VAT incl: NO, Shipping incl: YES).
  - Delivery time: 5-7 days.
- Sensy S-type load cell 2712
  - Price: 4 142 SEK/pc (VAT incl: NO, Shipping incl: NO).
  - Delivery time: 3-4 weeks.
- Futek LSB201
  - Price: 11 710 SEK/pc (VAT incl: NO, Shipping incl: YES).
  - Delivery time: 2 weeks.

Final Choice

The final choice relied on comparing the accuracy of each of the load cells as well as its price and delivery time. The characteristics are presented in 3.3.

Tab. 3.3: Load Cell specifications.

Manufacturer	**Model**	**Maximum Load [N]**	**Natural Frequency [Hz]**	**Fatigue Limit [cycles]**	**Nonlinearity [% of F.S.]**	**Hysteresis [% of F.S.]**	**Non-repeatability [% of R.O.]**
Interface	SSMF	500	>1500	107	0.05	0.03	0.02
Sensy	2712	500	N.S.	N.S.	0.03	0.03	0.015
Applied Measurements	DBE-50kg-003	490	>200	107	0.03		0.03
Futek	LSB201	445	8250	N.S.	0.1		0.05

N.S. = Not specified; F.S. = Full Scale; R.O = Rated Output

The final choice was the Applied Measurements DBBE-50kg-003-000. Firstly, for the price due to the need for two of these sensors. Secondly, because it has the best accuracy of the four and the smallest delivery time.

One possible problem could be the natural frequency. As stated in [17], "Most processing machines follow the rule that they operate without dynamic interference if their first natural frequency is at least 10 to 15 times higher than the fundamental excitation frequency of the drive mechanism.".

As the natural frequency of the sensor is 200Hz, 100 times higher than the expected excitation frequency of the system, it can therefore be considered suitable for the system being designed.

Friction Assembly Bearing selection

The selected sensor type possesses a distinctive feature with dual threads—one on the upper side and another on the lower side of the load cell.

A set of requirements has been established to ensure the safe installation of these sensors in the machine without causing any damage.

- The applied transverse load or bending moment shall be minimized to the sensors.
- The bearings and sensor, as a system, shall constrain one degree of freedom consisting of vertical movement.
- The bearings and sensor, as a system, shall have three degrees of rotation free between its ends.
- Both bearings shall be able to react to both negative and positive loads.

The following bearings were considered for the comparison:

1. Plain Spherical bearing rod end. Fig.3.27(a).
2. Ball Bearing rod end. Fig.3.27(b).
3. Self-aligning ball bearing. Fig.3.27(c).
4. Spherical roller bearing. Fig.3.27(d).

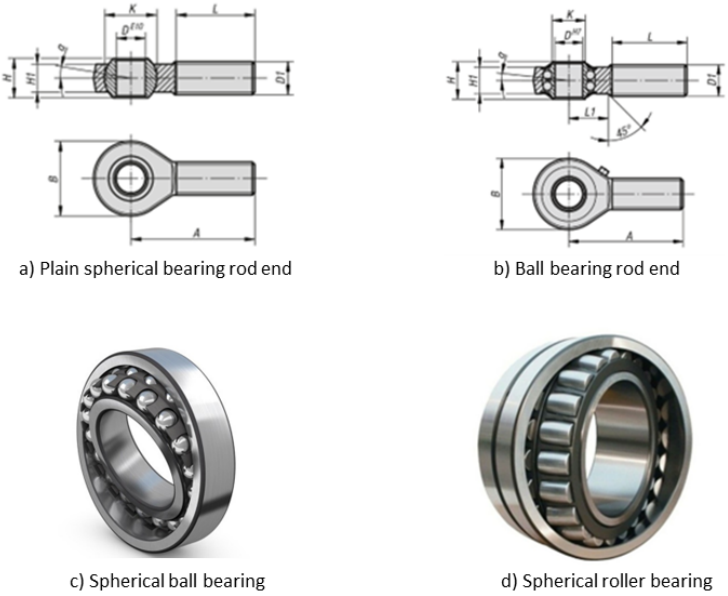

Fig. 3.27: Types of Bearings

Self-aligning ball bearings and spherical roller bearings share the drawback of requiring accommodation through additional components, thereby elevating system parts' overall count and cost. Additionally, the minimum diameter of these bearings is 20mm, which may pose challenges in accommodating them into the system.

The most straightforward and cost-effective resolution would involve the use of rod-end bearings. The distinctions between plain spherical and ball bearings primarily hinge on the misalignment angle.

The two types of rod ends of size M12 are compared as follows:

- **Misalignment** – The plain bearing has an allowed misalignment of 13 degrees, while the ball bearing rod-end has 7.5 deg.
- **Static Load** – The plain bearing has a load capacity of 23.5 kN, while the ball bearing rod-end has 1.8 kN. Both values are much higher than the expected load.
- **Internal radial clearance/play** – The plain bearing has a bearing clearance of 5 – 35 µm while the ball bearing rod-end has a value between 15 - 40 µm.
- **Compensation of internal radial clearance/play** - Compensation for internal radial clearance or play is crucial. Since a pre-load is applied to the assembly, this compensates for the internal clearances, ensuring accurate readings.
- **Friction values** – Despite efforts to obtain friction values from the bearing manufacturer, this information was unavailable. Typically, roller bearings are expected to demonstrate lower friction compared to plain bearings due to their reliance on rolling friction as opposed to sliding friction.
- **Price** – The plain bearing does not have a price of 140.70 SEK per bearing, while the ball bearing rod-end has a price of 479.18 SEK per bearing.

Considering these factors, a plain spherical rod end was deemed more suitable for the initial iteration of the test rig. If friction proves to be a concern, ball-bearing rod ends could be considered in subsequent iterations.

Housings

The housing assembly consists of a split housing with distinct top and bottom sections, the housing serves as the enclosure for the test bearing. The central bore within the housing aligns with a tolerance of H7, following the recommendations from the test-bearing manufacturer. Components of the friction sensor assembly are securely attached to the housing, responding to the friction torque generated by the bearing and thereby influencing the entire assembly. Inspired by its previous version, this housing iteration prioritises simplifications to facilitate machining, ultimately reducing lead time and overall costs refer Fig. 3.28. The split housing design is strategically adopted for effortless assembly and disassembly, promoting efficient maintenance and adjustments. Two dowel pins ensure precise alignment, while an NPT tapping is incorporated to accommodate a thermal probe.

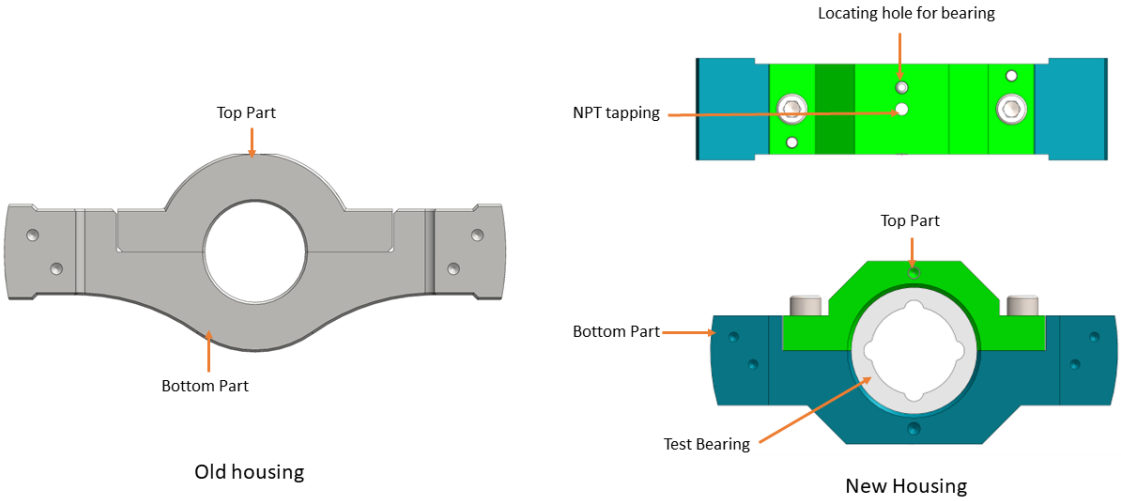

Fig. 3.28: Housing Comparison

3.4.4 Sealing system and tank

The tank consists of 2 main components: a custom water tank that will allow for the test-bearing to be submerged in water, and a shaft seal to prevent leakage from the shaft going through the tank.

Requirements

Requirements were set for tank and seal.

Tank Requirements

- Tank shall hold enough seawater to submerge the bearings under test completely.
- Tank shall have transparent walls to observe the test rig during operation.

- The front panel of the tank shall be easily removable to allow access to the bearings in between test without removing the tank.
- Front panel shall need to withstand the pressure of water with negligible leakage (less than 5g of water per hour of testing).
- Final design shall be easy to manufacture.
- Final design shall be affordable.

Seal Requirements

- Seal design should be as simple as possible.
- Seal should take up minimal space in the tank.
- Seal needs to be accessible from inside of the tank for ease of maintenance.
- Seal shall work with seawater.
- The seal shall apply minimal friction to the shaft.
- Front panel shall need to withstand the pressure of water with negligible leakage (less than 5g of water per hour of testing).
- Final design shall be affordable.

Tank Design

The design of the tank is displayed in Fig.13. It features a transparent acrylic body of pieces that will be bonded together. In the front of the tank a sliding removable acrylic panel provides access to the bearings under test. Knob bolts on the front face of the tank, will apply pressure to the front panel against a rubber gasket creating a watertight seal.

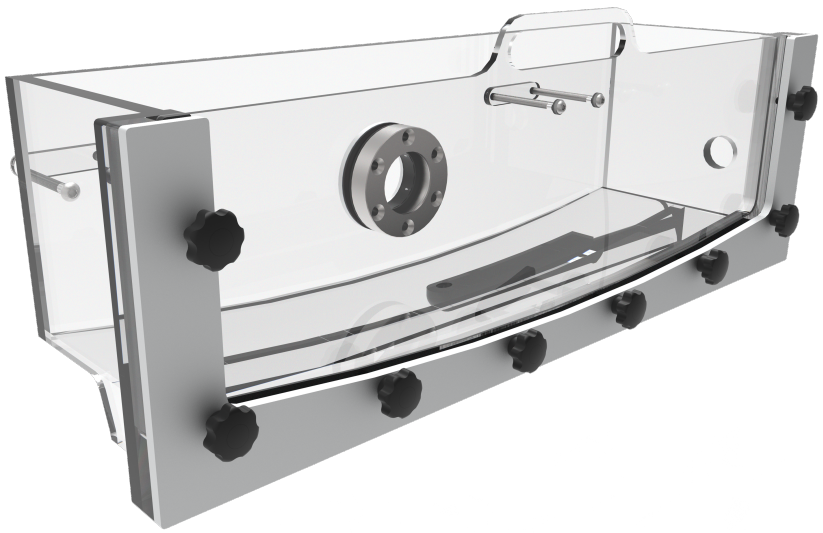

Fig. 3.29: Test rig Water Tank

The tank will rest on the testing rig with the back side fixed, mounting flush to the beam structure. The bottom of the testing rig is made from acrylic as well and is curved to fit around the existing geometrical constraints of the testing rig. A drain hole is also provided on the bottom of this sheet and will be connected to a 3D-printed drain extension below the tank and will be attached to a plastic hose using a brass male coupler nipple. On the end of this hose, there is a brass two-way ball valve that can be opened to allow for water to pass through. Additionally, a 32mm hole and concentric mounting holes are allocated for the seal and housing configuration. These are oversized to allow for fine adjustment of the seal after the tank has been installed.

The material chosen for the tank is a combination of acrylic and aluminium. Acrylic is impact-resistant and transparent, making it a commonly used material for the design of testing rigs and pressure test chambers. Aquariums are commonly made from bonded acrylic, so the design is resistant to seawater and corrosion. Aluminium is another material chosen for our design; the non-ferrous material will not rust when subject to seawater, however, it may cause some galvanic corrosion after extended periods. Because aluminium is affordable, we have chosen to use aluminium in locations where it is not directly exposed to seawater.

Water Tank Manufacturing

Steps were taken to ensure the simple manufacturing of the tank. All acrylic pieces are designed to be laser-cut with no machined cuts or extrusions. Manufacturing could be completed on campus using available materials and equipment.

To assemble the tank the bonds between the acrylic and aluminum pieces would be glued together using a two-component epoxy glue called Power Epoxy from Loctite. This two-component epoxy glue had a curing time of 5 minutes which gave enough time to assemble without waiting too long to assemble the rest of the pieces.

Seal Design

Several different sealing solutions were investigated for this case including:

- Rotary Lip seals
- O-ring lip seals
- Packing seals
- Mechanical seals

When investigating Mechanical and Packing seal solutions it was realized that there were no options for seals for our dimensions that would fit in the limited space that exists between the test-bearing housing and the support bearings. These solutions are also complex thus they do not meet the criteria of being easy to assemble and disassemble and ease of maintenance which is a major requirement. For these reasons, Mechanical and Pacing seals have been disregarded and instead, custom sealing designs using standard Radial lip seals and O-ring lip seals were decided to use.

Three different solutions were developed that best suited the present use case, these were using an O-ring lip seal, using two Rotary oil seals with a grease chamber, and using a single greased Rotary oil seal.

The O-ring sealing solution provides a slim solution with good sealing capabilities, the dual Rotary oil seal with a grease chamber provides excellent sealing properties and low friction and the single Rotary oil seal provides low friction and good sealing properties.

Dual Rotary Oil Seal Solution

Rotary oil seals are designed for oil and thus there is an uncertainty on how well it would work with sealing saline water. For this reason, using saline water as the only sealing medium for this type of seal would risk that the solution would not work well enough to satisfy our requirements. One solution that makes it possible to use Rotary oil seals in this application is to use two seals and a chamber of grease as seen in Fig. 3.30.

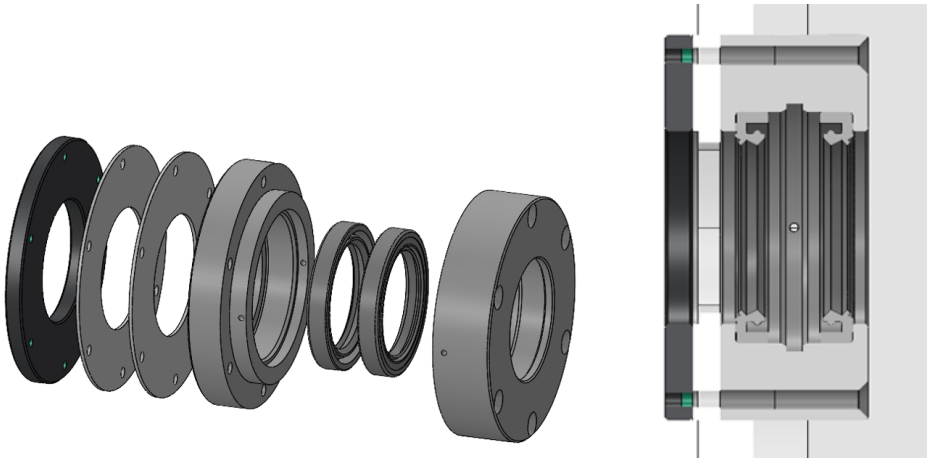

Fig. 3.30: Dual Rotary Oil Seal Solution

The Rotary oil seals would be facing the chamber and the grease making it the main sealing medium, this means that the seals would keep the grease from escaping the chamber successively sealing the tank. This type of sealing solution are also implemented for dry running seals in vacuum/air sealing functions ans seen in figure 3.31.

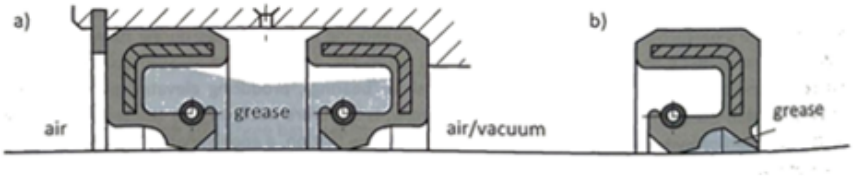

Fig. 3.31: Dry running sealing solutions in Vacuum or Air Functions [12]

The system would be using two housing pieces that will house the seals thus creating the chamber with oil while allowing for the shaft to go through. The system will be held together as well as to the tank with the help of M5 screws that go through the housing pieces and screw in to a back plate on the dry side of the tank as seen in Fig. 3.30.

The advantages and disadvantages of this sealing solution are:

Advantages

- Minimal Friction
- Minimal water leakage

Disadvantages

- Possibility of contaminants
- Bulkier design

Leakage was found to be small for this sealing solution as in the leakage control test which adheres to the DIN 3761 standard the maximum allowed leakage for every seal design was determined to be 1-3 g of oil for a 240 hour test. As the test rig test cycles are going to be shorter than the DIN 3761 standard test [18]. Regarding the possibility of grease leaking in to the water, when technicians at Trelleborg AB were consulted it was indicated that there is a greater possibility of the water leaking in to the grease chamber than the grease contaminating the water. This is due to the short test cycles that will be conducted.

Two seal manufacturers were considered to provide the seals for this solution which were Trelleborg AB and SKF. Both of these manufactures have a wide variety of industrial Rotary oil seals, the companies were also consulted to chose an appropriate seal:

Trelleborg TREB00300

- Seal is made from Fluorocarbon rubber (FKM) which is resistant to seawater.
- Maximum pressure is 0.05 MPa.
- Maximum speed is 10 m/s.
- 7 mm width.
- Applicable for oscillating shafts.

SKF HMSA10 V

- Seal is made from Fluorocarbon rubber (FKM) which is resistant to seawater.
- Maximum pressure is 0.05 MPa.
- Maximum speed is 14 m/s.
- 6-8 mm width.

Single Rotary Oil Seal Design

The sealing effect of Rotary oil seals with saline water as the main sealing media in dry running conditions is unknown. By greasing the the space between the dust lip and the main sealing lip as seen in Fig. 3.31 as in dry running in vacuum/air sealing functions [12], this seal type can be an option for this application. This system made use of one housing to house the seal which is turned towards the saltwater making it the main media for sealing. The seal housing will be fitted to the tank with the help of six M5 screws that will go through the housing and attach to a back plate with threaded holes as seen in Fig. 3.32.

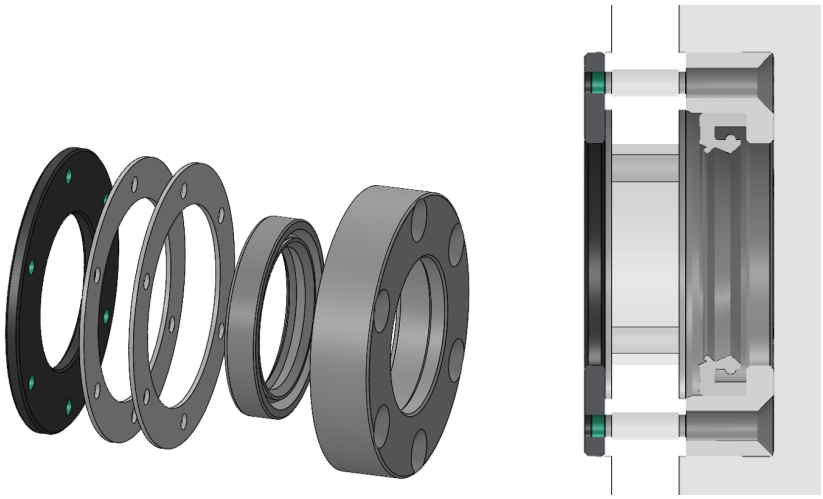

Fig. 3.32: Single Rotary Oil Seal Solution

The advantages and disadvantages of this sealing solution are:

Advantages

- Low Friction
- Slim Design
- Uncomplicated design

Disadvantages

- Possibility of contaminants
- Presence of some leakage

As these seals were not designed for water applications there was uncertainty about how well it would work and how much water leakage was to be expected. As the small space between the main lip and the dust lip would be greased there could be contamination in the water.

Two seal manufacturers were considered to provide the seals for this solution which were Trelleborg AB and SKF. Both of these manufacturers have a wide variety of industrial Rotary oil seals, the companies were also consulted to choose an appropriate seal:

Trelleborg TREB00300

- Seal is made from Fluorocarbon rubber (FKM) which is resistant to seawater.
- Maximum pressure is 0.05 MPa.
- Maximum speed is 10 m/s.
- 7 mm width.
- Applicable for oscillating shafts.

SKF HMSA10 V

- Seal is made from Fluorocarbon rubber (FKM) which is resistant to seawater.
- Maximum pressure is 0.05 MPa.
- Maximum speed is 14 m/s.
- 6-8 mm width.

O-ring Lip seal Solution

The O-ring lip seal solution was developed in discussion with the technicians at Trelleborg. They suggested that a Roto VL sela solution. This is an uncomplicated design with a housing that holds the seal and is attached to the tank with M4 Screws that go through the housing and screws into a back plate on the dry side.

This solution was a suggestion by the technicians at Trelleborg AB who were consulted during the development of the seal. The Roto VL Seal was suggested to use which is a lip seal that is pressed on the shaft using a o ring. This was an uncomplicated design with a housing that holds the seal and is attached to the tank with M5 Screws that go through the housing and screws into a back plate on the dry side as seen in Fig. 3.33.

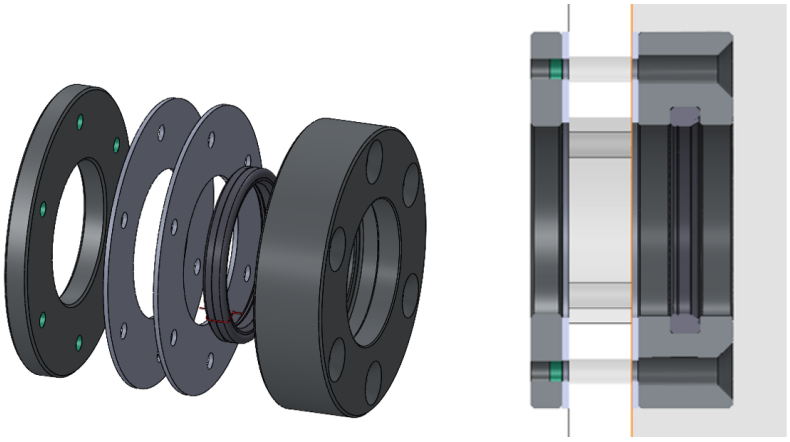

Fig. 3.33: O-ring lip seal solution

The advantages and disadvantages of this sealing solution are:

Advantages

- Slim Design
- Uncomplicated design

Disadvantages

- Higher friction
- Presence of some leakage

The technicians at Trelleborg predict that there would be a thin film of leaked water on the dry side, this film would be managed by a drip plate and a rubber brush barrier or an o-ring divider that will stop the water. The magnitude of the leak depends on the system around it and it cannot be predicted how thick the film will be with certainty. This seal will also cause more friction, which will not affect the final readings of the sensors.

For this solution Trelleborg AB is the company to provide the seal, this is because they suggested the idea and helped with its development:

Trelleborg TE1200300

- Seal is made from Fluorocarbon rubber (FKM) which is resistant to seawater.
- Maximum pressure is 30 MPa.
- Maximum speed is 2 m/s.
- 4.8 mm width.
- Applicable for oscillating shafts.

Chosen Sealing Configuration

It was decided that the Single rotary sealing solution as seen in Fig. 3.32 would be applied to the design. The reason for this selection was because if its simple design which is the easiest out of the three solutions to manufacture thus cutting the cost and lead time. Concerning the possibility of the water being contaminated with the grease, it had been decided to test the seal without greasing it and evaluate the amount of leaking. If the leaking is not of a satisfactory amount a grease that would minimize the risk of contamination would be sourced.

3.4.5 Electronics and DAQ

The power supply and the Data Acquisition system (DAQ) are based on the wiring and coding made for the initial test rig. The test rig is plugged into an electronic box. This box aims to supply the power needed to drive the motor to the sensors and gather the signal from the sensor to send it to the DAQ.

Part of the electronic box components are used to control the oil pump which was included in the initial test rig. This oil pump is not of interest to our design. Therefore, the cables linked to its utilization have been unplugged, and this system will not be used.

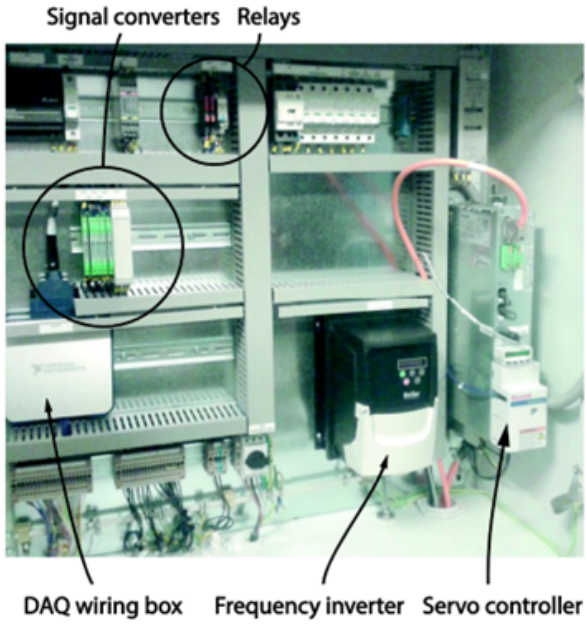

Fig. 3.34: Electronic box - Photo

The power supply part of the wiring is going to be reused as such. The motor can be controlled the way it is needed and different safeties and an emergency button are already included.

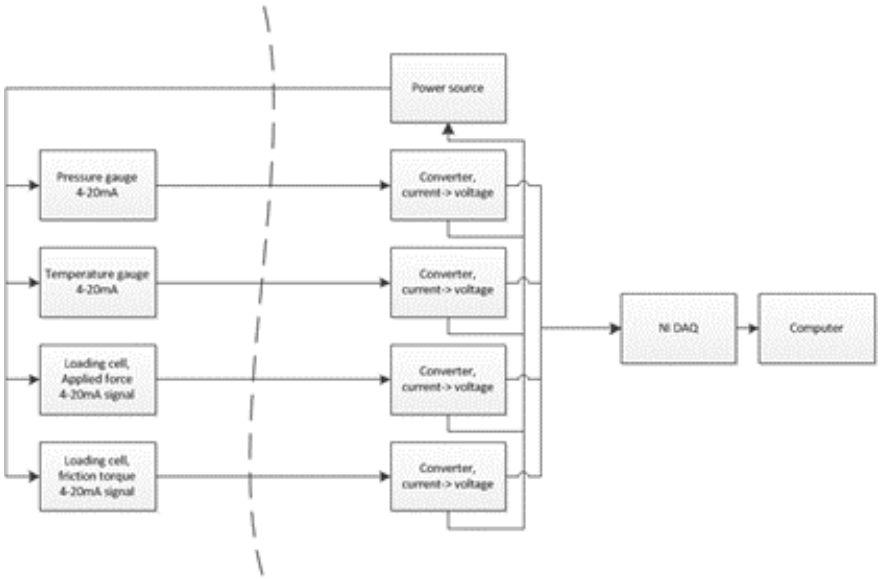

Fig. 3.35: Electronic box - Graph

All the sensors are connected to the National Instruments SCB-60A Connector Block. This block is then connected to the computer via a cable. This block allows for both analog and digital connections and its use is straightforward.

To read the data from the Connector Block, three possibilities were evaluated: Python, Matlab and LabView. Before the current project, the data acquisition was being performed using Matlab and Python. However, the files that were in the computer associated to the rig were not working

properly.

Each possible solution presents advantages and disadvantages.

Firstly, Python has the advantage of being highly flexible and several packages can be used in general and there are some toolboxes developed by Bosch Rexroth to control the motor using Python. However, due to the lack of knowledge and low comfort in using this tool, it was discarded.

Secondly, using Matlab's Data Acquisition tool allows the reading and saving of the data of the sensors, but does not allow the easy manipulation of the data (at least to the extent of the knowledge of the group members). This aspect wouldn't allow a quick set-up of the pre-load of the sensors. Another aspect lacking in Matlab is a toolbox or add-on to connect Matlab to the motor control unit. Not being able to read and save the data of the encoder or to control and save the data from one place only can be seen as a limitation in future developments of the machine. One good aspect of Matlab is the easy and direct reading of the voltage of the sensors.

Lastly, LabView is a tool developed by National Instruments that does not require too long of an adaptation (block coding) and it was already installed on the computer. It allows both the data manipulation and instant saving and visualization of the results. It is also a tool that is being used in the Machine Design Department. The main disadvantage is that although add-ins exist to connect LabView to the motor control unit, they are more suitable to be used in more recent versions of LabView. A connection was attempted using the LabView 2018 version but without much success. Updating it to a newer version will allow for it.

The software that was chosen was LabView. It allowed for a quick, simple setup and a prospective long-term use. As a fallback, Matlab can be used to ensure that the voltage readings are correct.

Different code versions were saved on the computer. The associated 'README.txt' file presents a quick explanation of the developments and state of each one of the versions. No code management tool (Git) was used during the project, so every version was saved separately.

The objective during the development of the code was to leave a Minimum Valuable Product (MVP) able to be scaled in the future.

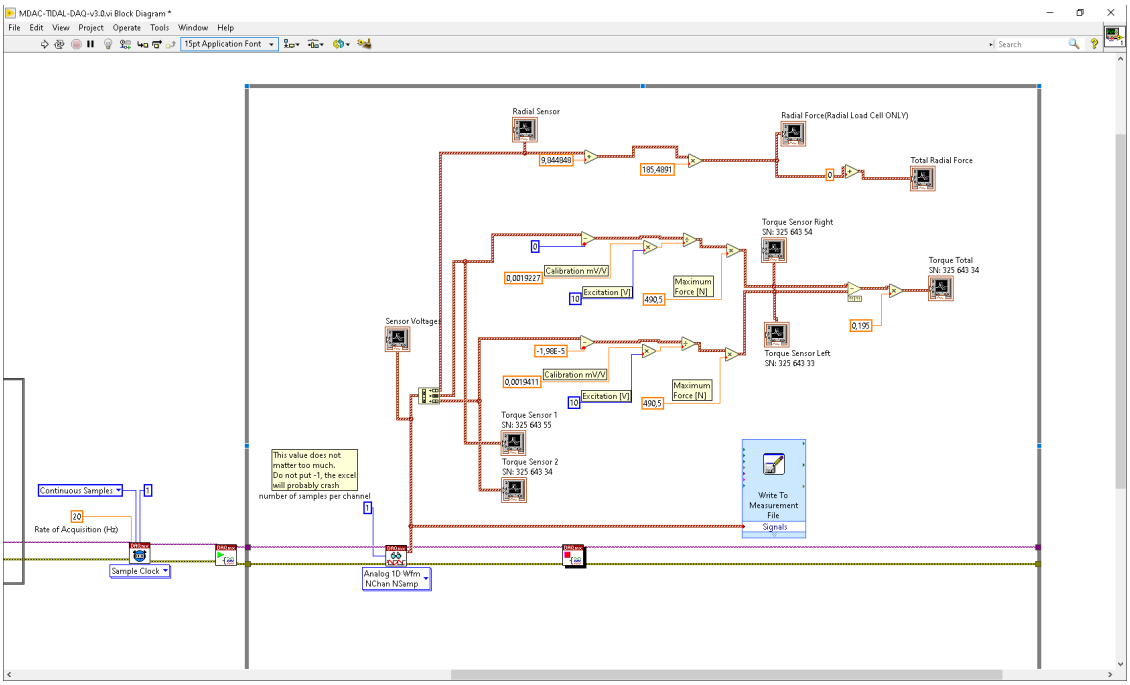

Fig. 3.36: Part of the block Diagram of version 3.0 of LabView

The last version of the software (v3.0) has the following characteristics:

- It uses the data of the two load cells used to measure friction ($0 - 20mV$, when exited with $10V$) as well as the data from the load cell used to measure the radial load applied by the lever arm system ($-10 - 0V$).
- Manipulation of the data of the two load cells used to measure friction according to the load cell manufacturer calibration file, see Fig. 3.36
- Visualization of the voltage of the three sensors, visualization of the force of the two load cells used to measure friction.
- A graph with the radial load (not working properly).
- Saving of the voltages of the three load cells in a '.tdms' file. Two main features associated to this were ensured: (1) the files were not overwritten and (2) that more files were created once the previous got filled with data (especially important in long duration tests). This .tdms files can easily be opened using Excel and the respective National Instruments add-on (refer to the National Instrument's website on how to install and read this file).

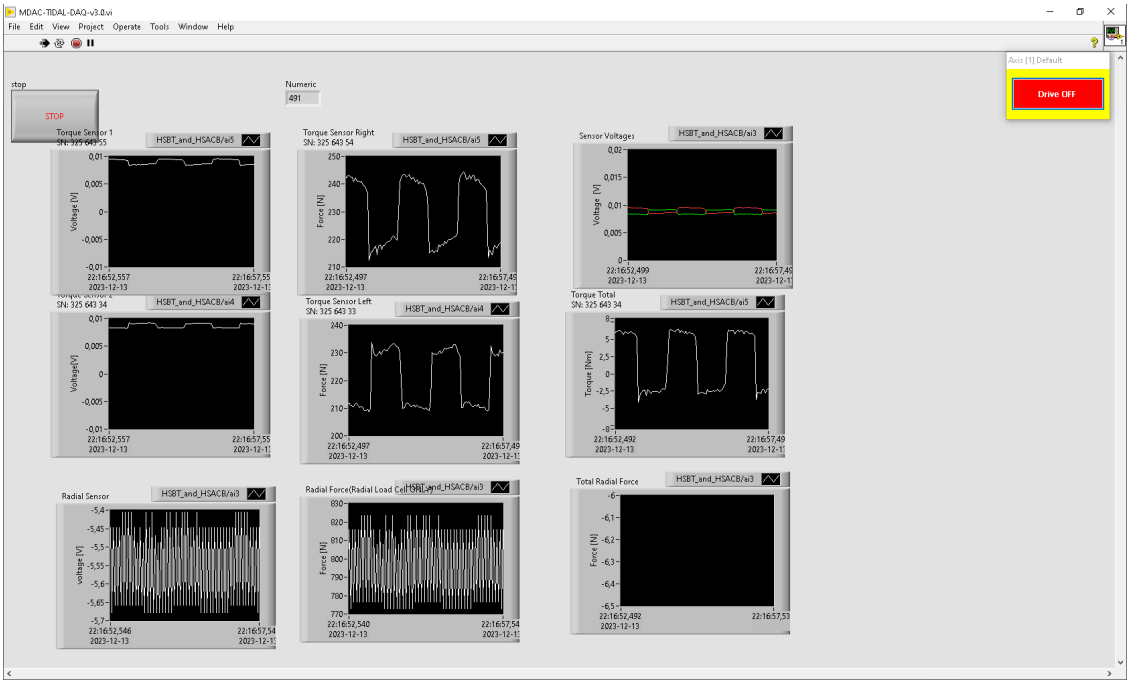

Fig. 3.37: Front Panel of version 3.0 of LabView

This version has a big room for improvement as it is very rudimentary. The radial force is not being correctly manipulated, see Fig. 3.36 and Fig. 3.37. This is due to the stabilization effect and resolution that is being performed by the amplifier and digital screen associated to this load cell. More time needs to be put in understanding and configuring this modules.

With the radial load being visualized using the LED number display it was possible to know the radial load applied (it varied during the test and that variation was not fully possible to be measured).

Some problems were faced in version 2.3. The constant values entering the 'Sample Clock' block and the 'Analog 1D (etc.)' block were higher than 1 so there was a delay between the sensors. This was fixed after the first long test in version 3.0. In Chapter 6, the solution in the pos-processing is going to be described.

Motor control

To control the motor, the program 'IndraWork DS' was used. This program allows the full control of the motor, visualization and description of the errors, visualization of some parameters (using the Oscilloscope mode) and configuration of the ports.

The control of the motor can be done in two ways: (1) constant velocity, using the 'Optimization / commissioning –> Easy startup mode' or (2) reciprocating motion using both the 'Optimization / commissioning –> Easy startup mode' to enable the motor control and the 'Optimization / commissioning –> Command value box' to define the reciprocating motion parameters.

Chapter 4

Proof Of Concept

Delivery estimates for manufacturing the stainless-steel shaft, and other critical components exceeded the time frame of the project. Modifications to the final design were added to accommodate an accelerated manufacturing timeline. These modifications, along with much of the original design, were manufactured, assembled, and tested to prove the validity of the test rig concept.

4.1 Modifications to Final Design

The previous testing rig discussed in section 2.1.1 has a steel shaft. This will corrode in saline water, so it is not a permanent solution for this testing rig. However, for short initial tests, it is sufficient to understand if the measurement system will function as intended. The design of the previous shaft is similar but has an 8 mm keyway instead of a tapered end. The sleeve was adapted to support this keyway shown in Fig. 4.1 and Fig.4.2.

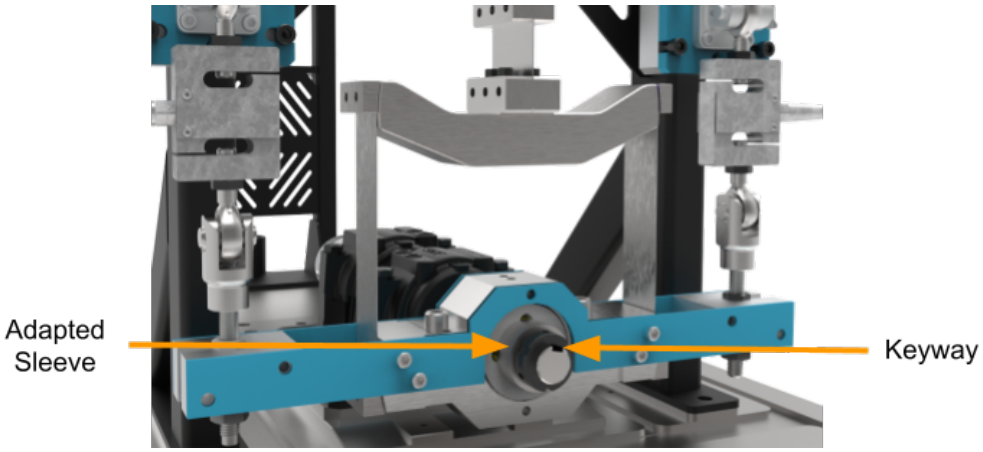

Fig. 4.1: Adapted final test rig design

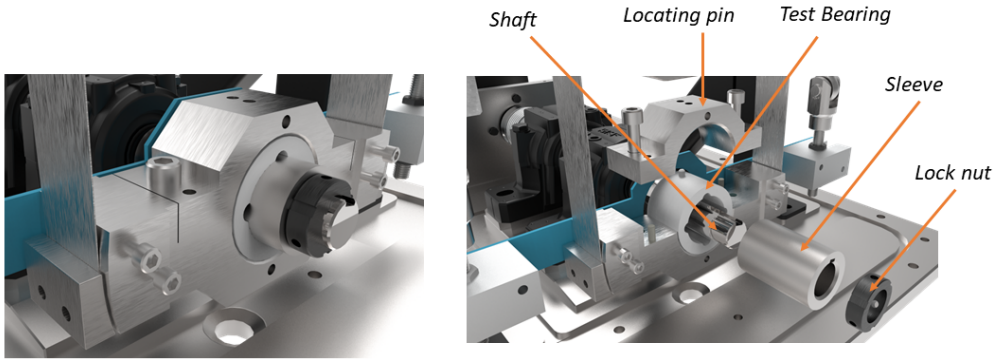

Fig. 4.2: Adapted Shaft and sleeve assembly

In addition to the sleeve, the seal had to be redesigned to accommodate the existing space and diameter of the shaft. The existing shaft had a diameter of 39 mm and a hardened surface with poor surface quality. Generally, high surface quality and surface hardness are necessary for lip-sealing solutions to prevent leaks. For this proof of concept, the objective seal is to get a measurable leakage rate of less than 1 ml per hour. This standard is based on space for a drip plate or cloth to catch water during a long-term test.

The seal was chosen from a supplier Remlaget and is a non-standard generic rotary seal; this is a similar design recommended by local companies SKF and Trelleborg for the test rig's specific application. Those companies did not offer this type of seal in the 39mm size required for the existing shaft. Dimensions of the seal housing, gaskets, and tank backplate were modified to support the new size and shape of the seal.

4.2 Manufacturing

Components were divided into two categories for manufacturing: outsourced and made in-house. Outsourcing was reserved for parts with high tolerance requirements, CNC Machining or atypical materials, such as stainless steel, which cannot be manufactured at KTH Prototype Centre. The two components that were outsourced were the bearing bottom and top housings refer Fig. 4.3. These parts were manufactured in stainless steel and have H7 tolerance on the bore that seats the bearing. The remainder of the custom parts for the friction measurement assembly Fig. 4.3 were manufactured at KTH in either aluminum or mild steel. Some mild steel parts were painted blue to prevent corrosion. The acrylic and rubber pieces for the tank were manufactured using the laser cutter in the prototype center.

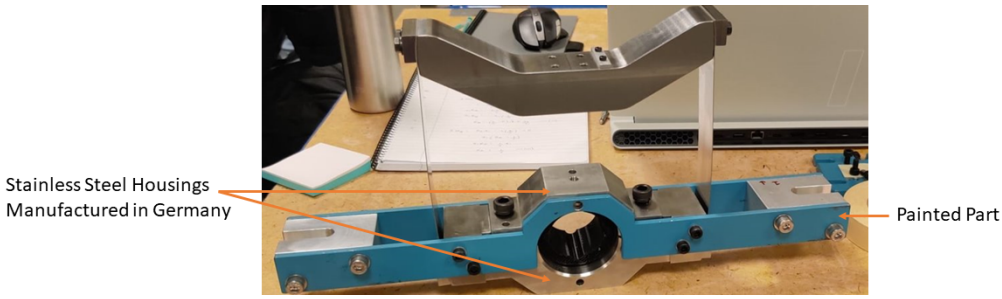

Fig. 4.3: Maufactured parts

4.2.1 3D Printed Prototypes

Extended lead times were encountered for outsourced products like Load Cells and Vesconite test bearings. In response to this challenge, 3D printed prototypes of these components were produced utilising the 3D printers available at the KTH prototype centre. This approach aimed to mitigate any disruptions to assembling components interlinked with these parts. Fig. 4.4 shows the different components that were 3D printed and further integrated into the system.

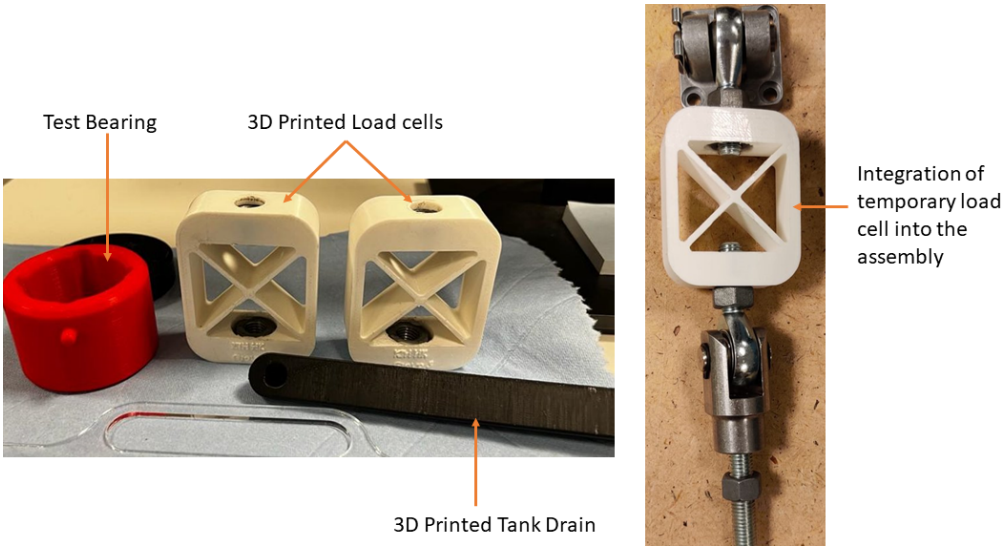

Fig. 4.4: 3D Printed Parts

4.2.2 Tank

A 2-part epoxy was used to bond the acrylic and aluminum structure of the tank. This was due to constraints within KTH that prevented the shipping and receiving of glues. The assembly was limited to the best glue available in local hardware stores. Acrylic cement is the preferred alternative, resulting in much stronger, cleaner, and waterproof bonds.

The tank was assembled in the following order. If a 2-part epoxy is used for acrylic bonds, it is critical to sand all contacting faces before glue is applied. Throughout the process wipe off any excess glue.

The steps for manufacturing the tank are as follows:

1. Apply 2-part epoxy to the face of the 2 ribs and bend the bottom tank sheet to fit the shape of the rib.
    - Use the curve of the backplate and weights to apply pressure to the glue joint. Ensure the entire length of the backplate has contact with the ribs.
2. Sand the side of the glued assembly until the sides of the rib and bottom plate are flush.
3. Individually glue each side of the tank.
    - Use a square to ensure the sides are angled at 90 degrees.
    - Clamps can assist in holding the tank together.
4. Glue on the backplate.

- Ensure it is aligned correctly using a square.

5. Sand the contact edges opposite of the backplate so all edges are flush.
6. Using a 2-part epoxy, glue the aluminum pressure plate to the acrylic sliding support part.
7. Glue the connector panel to the sliding support part.
8. Glue the two assemblies together.
    - Ensure both assemblies rest flush on the bottom.
9. Wait 24 hours, or a sufficient time for the glue to fully cure.
10. Apply silicon using a caulk gun to the inner edges of the tank.
11. Evenly smooth the silicon after application.
12. Using a 2-part epoxy, glue the 3D-printed drain part to the bottom of the tank, aligned with the drain hole.
    - Ensure the fitting connection has no leaks before it is attached to the tank.
13. The manufactured tank is shown in Fig.4.5

Fig. 4.5: Manufactured Tank

4.3 Assembly Instructions

4.3.1 Shaft Installment

The shaft was installed in the following order.

1. Support Bearings with the respective sleeve assembly are pressed onto the Shaft.
2. Shaft installed into the bottom half of bearing housing.

3. The axial position of the Shaft is aligned with the CAD model; the positions of the bearings are shifted as needed.

4. Bearings are locked into place with a lock washer and a coupler is connected between the motor and shaft.

5. Seals are inserted appropriately into the support housings.

6. The locating rings are inserted in the roller bearings support housing.

7. LGHB 2/ 0.4 SKF grease is applied to the bearing. Refer to Fig. 4.6.

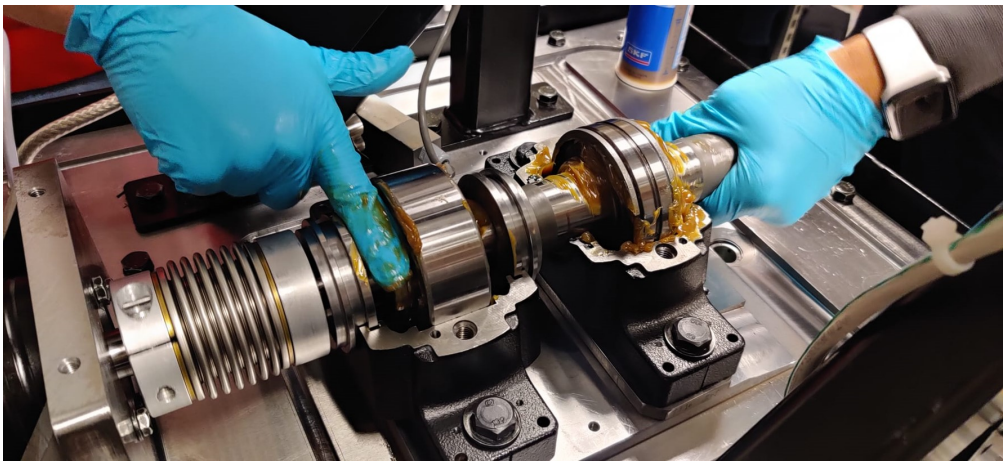

Fig. 4.6: Applying grease to support bearings

8. The top of the bearing housing is bolted down.

9. Use a dial gauge to verify the proper installment of the shaft. Conduct a sweep test to check the run-out of the shaft.

   (a) Install a dial gauge so it is just touching the surface of the shaft similar to Fig. 4.7.

   (b) Enable continuous shaft rotation at 10 RPM. See section 5.1.2 for how to enable motor controls.

   (c) Note the deviations picked up by the dial gauge. Ensure deviation is less than 50 µm throughout a full rotation.

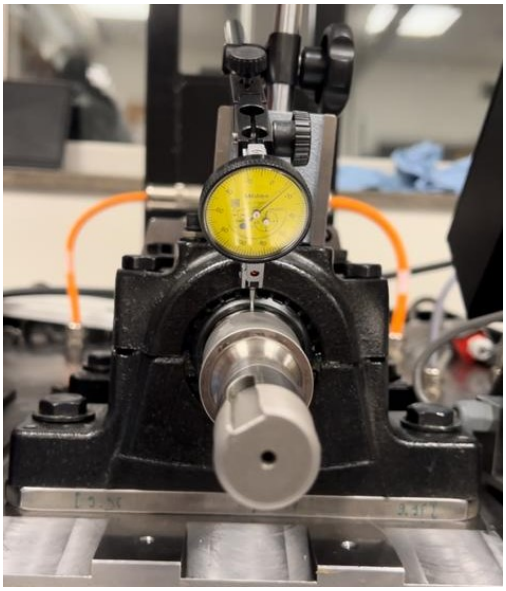

Fig. 4.7: Sweep test on installed shaft

4.3.2 General Assembly

The assembly of the testing rig is straightforward and follows the CAD files. Assemblies in Fig. 4.8 were built concurrently to match the CAD model. A 3D-printed sensor component was used for initial assembly to prevent damage to the sensors. This was replaced once the DAQ system was functional.

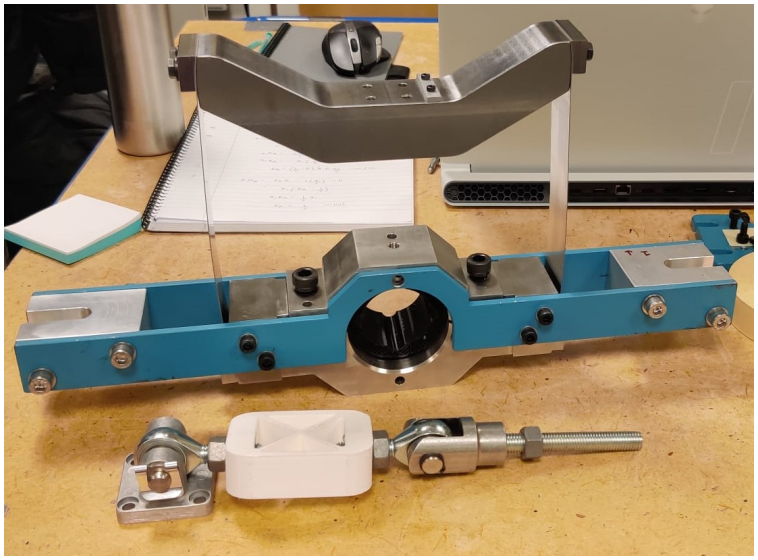

Fig. 4.8: Sleeve housing (top) and temporary sensor (bottom) assemblies

The parts are mounted in the following order:

1. Install shaft according to section 4.3.1.
2. Install clevis brackets and associated mounting plates to the structure of the testing rig. Make fine adjustments to ensure they are aligned vertically and horizontally on each beam.

3. Install tank and seal assembly onto the shaft flush with the face of the test rig structure.
4. Fix tank to test rig structure. Ensure seal housing is concentric with the shaft.
5. Insert the sleeve housing and tension sheet assembly (Fig. 4.8 top) concentrically with the shaft. Attach to the lever arm and tighten screws as necessary to remove slack.
6. Use the pins in the rod ends to attach the sensor assembly (Fig. 4.8 bottom). Route the threaded rods through the aluminum slot and add a nut. Do not tighten.
7. The completed assembly is ready for test setup and should match Fig. 4.9.

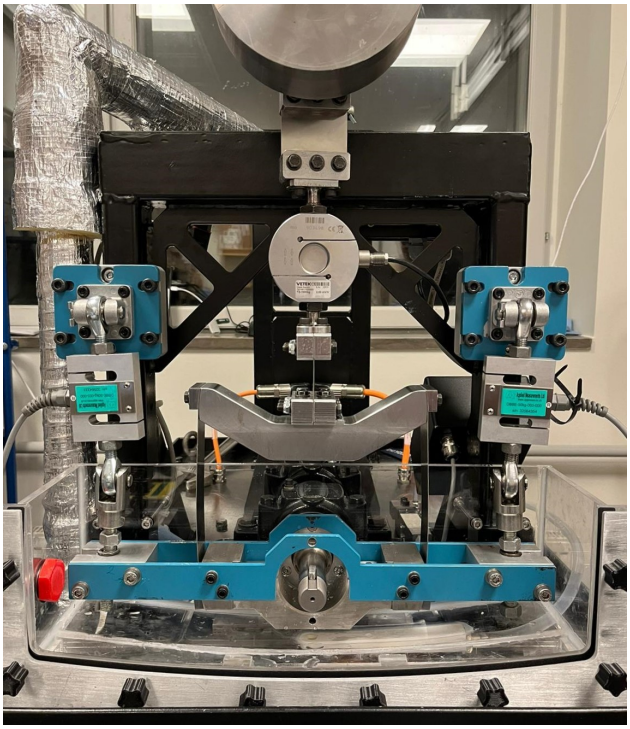

Fig. 4.9: Completed assembly of test rig

Chapter 5

Setup Process

5.1 Machine Electronics Setup Procedure

This section outlines the procedure for connecting the test rig to the computer. The steps presented include securing power connections, establishing communication interfaces, initiating the motor, and configuring the Data Acquisition (DAQ) system.

5.1.1 Connections

The test rig should be connected to the power source and the computer to operate. On the computer side, it should be connected to the National Instrument box and the motor controller. All the connections needed are illustrated in Fig. 5.1.

(a) Power plug connection

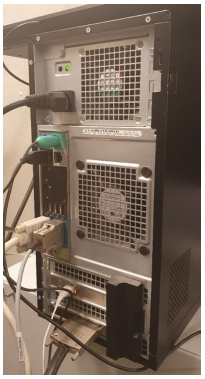

(b) Computer connections

(c) Motor connection

Fig. 5.1: Connection example

5.1.2 Turn on the Motor

After plugging the main power cable, the main switch and all the relay switches need to be turned ON. After that, the fan will start to turn and the motor controller display is now visible.

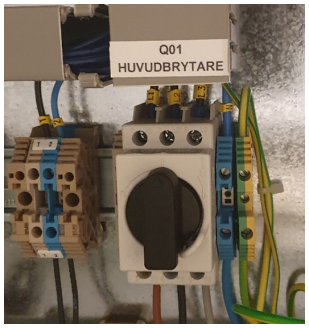

(a) Main switch

(b) Relay switches

Fig. 5.2: Wire box switches

At this point, the blue button in the emergency block turns on. This button is used to reset the circuit. Press the button to reset and if all the breakers are engaged and the red stop button is not activated, the blue light disappears and the machine is ready.

Fig. 5.3: Emergency stop block

If the blue light doesn't disappear, it means that the little security key is missing. This security was used when the test rig was equipped with a protection cover that needed to be clipped. The key can be added and the blue button should now glow.

Fig. 5.4: Security key

5.1.3 Data Acquisition Software

To start the data acquisition, the following procedure must be followed:

1. Turn on the computer.
2. Log in with the credentials (Password: New4you2020).
3. Turn on the power supply of the Load Cells (10V).
4. In the Desktop environment, find the folder 'MDAC-Tidal-Turbine-Bearing/LabView/v3.0 (or similar).
5. Open the LabView file in the folder. LabView 2018 x32 should start. After some seconds, the front panel of the program should appear.
6. Double-click on any of the graphs. The block diagram associated with the previous step is now open.
7. Double-click on the 'Write on Measurement File' block. A window will appear.
8. Edit the path and name of the file to store the data that is going to be acquired.
9. Click 'OK'. Repeat the two previous steps to ensure that the path was changed.
10. Close the window.
11. The sample rate can also be changed in the block diagram window.
12. Click 'Crtl+S' or save in 'File –> Save'.
13. Close the block diagram.

14. On the Front Panel, click on the white arrow on the top left of the screen. The data is now being recorded.

15. Open the folder where the data is going to be saved and ensure that a new file has been created and its size is increasing.

16. Change the scale of the graphs in the Front Panel in order to see the data being read.

After this step, the data is recorded and the motor control can be activated.

5.1.4 Motor Control

To control the motor, the following steps shall be followed:

- Open the IndraWorks app which is already pinned in the taskbar of the computer.
- The first window that appears is the Communication Window. Here the correct COM port needs to be selected, as well as the Baud Rate. Select COM1, a 'Timeout' of 205ms, a 'Baud Rate' of 115200 (default) and 'None' in the 'Parity'. See Fig. 5.5.

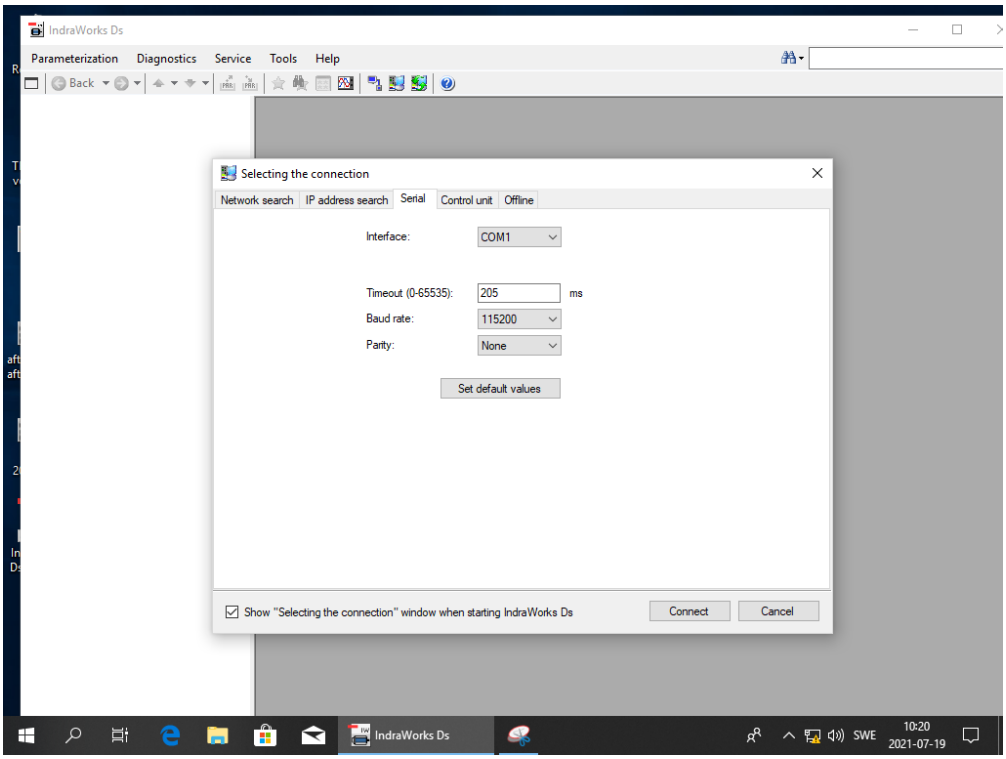

Fig. 5.5: IndraWorks communications window

- As a good practice, the encoder value should be reset. Go to the symbol of the motor with a red arrow pointing down and select the respective option to reset the encoder value.
- On the left side, there are several command folders. In order to start the motor, select 'Optimization / commissioning' and 'Easy startup mode'. A window like the one in Fig. 5.6 should appear.

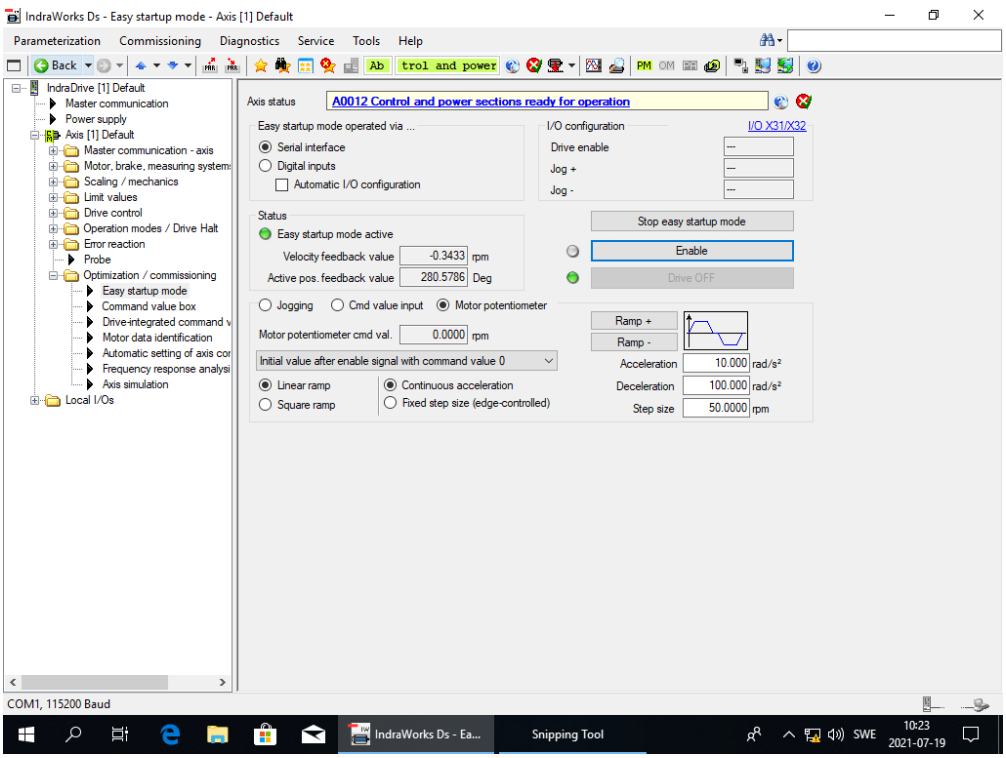

Fig. 5.6: IndraWorks startup mode

- If the 'Turn on the motor' procedure is followed, then the 'Start easy startup mode' button must appear. Click on it. A warning window similar to the Fig. 5.7 appears. Ensure that the emergency button is in hand. Check that all the other pre-requisites mentioned in the warning are being met and click 'OK'.

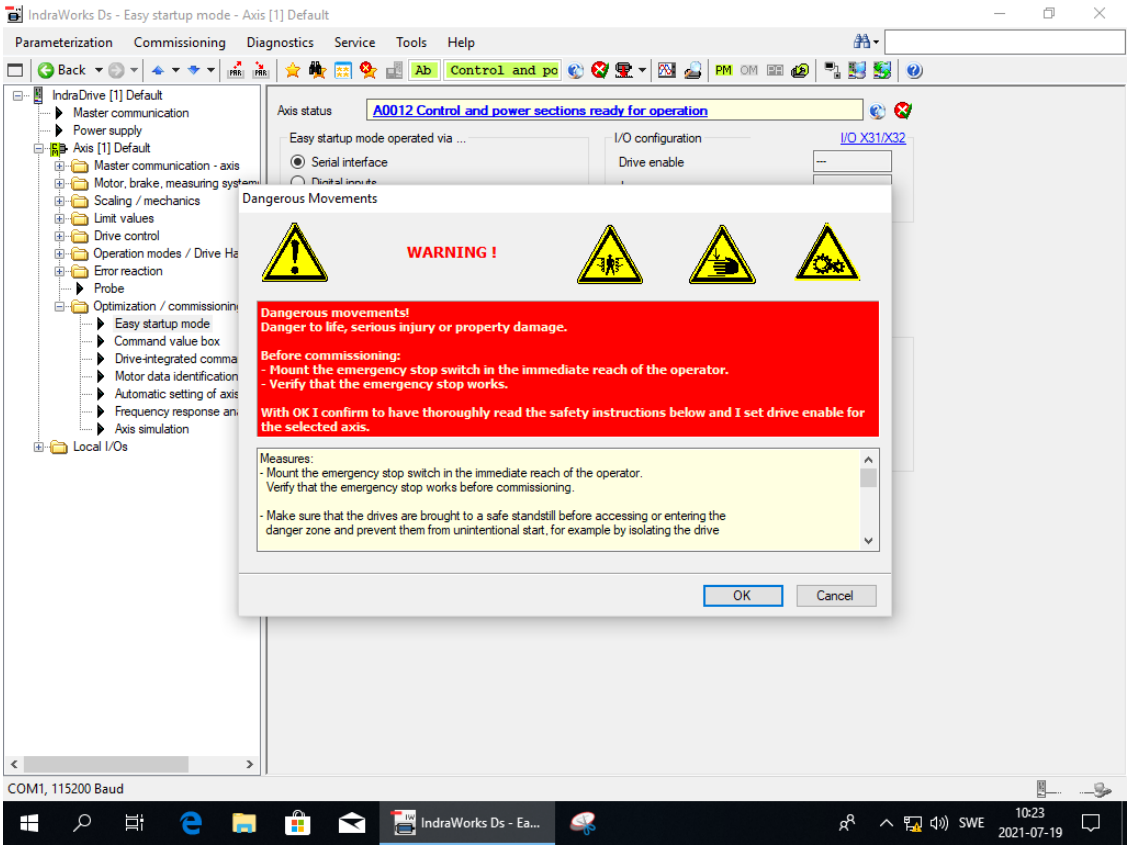

Fig. 5.7: IndraWorks Warning Window

- On the left, below 'Optimization / commisioning' click on 'Command value box'. A window similar to the Fig. 5.8 should appear.

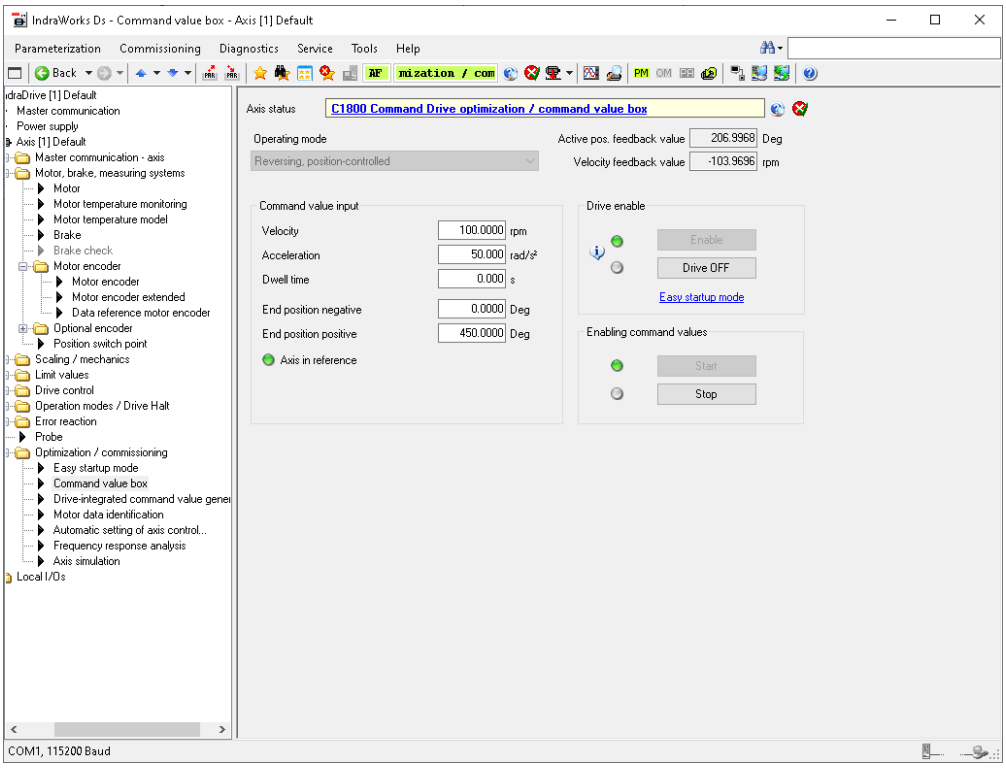

Fig. 5.8: IndraWorks Command Box Control

- Change the parameters to the values intended for the test. Be aware that attached to the motor there is a gearbox with a ratio of 5, therefore all values intended for the shaft related to angle, velocity and acceleration should be multiplied by 5 and all the torque and power values (in case of choosing other control options) should be divided by 5.
- Click 'Enable' and 'Start'. The motor should now start moving
- In case of emergency, the physical emergency button should be pressed. Another way involves pressing 'Drive Off' button on the software.

5.2 Test Setup Procedure

The following procedure is required each time a new test is conducted. Fig. 4.9 demonstrates the configuration the test rig should be in at the start of the test setup procedure.

1. Install test bearing into the housing. Fit the pins in the guide holes similar to Fig. 5.9a.
2. Install sleeve on shaft, fixed in place with shaft key.
3. Lock the sleeve in place using the locknut similar to Fig. 5.9b.
4. Install the top bearing housing piece as shown in Fig. 5.9c to hold the bearing in position.
5. Set up dial gauge on the sleeve as shown in Fig. 5.9d.
6. Apply radial load until contact is made between the bearing and sleeve, which is ensured by the dial gauge
7. Apply the radial load to the desired value (<5kN). Use the digital readout shown in Fig. 5.9e on the back of the test rig as a guide.
8. start DAQ system and produce a live readout of loads on the left and right load cells. More details instructions are in section 5.1.3.
9. Tighten nuts shown Fig. 5.9f in to apply a 250N preload to each load cell. This should be done slowly using the DAQ system as a reference for how much the nuts need to be tightened. Due to misalignment, there may be a difference of 10 N between the load cells, which can be accounted for in post-processing.
10. Install the front panel of the tank similar to Fig. 5.9g.
11. Fill with water and assess if there are any leaks. Address significant leaks before the test is conducted. Minor drips can be accommodated with a drip plate or cloth.
12. Set up test parameters including motor speed and reciprocation characteristics in the menu on Fig. 5.9h. More details instructions are in section 5.1.4.
13. Begin test.

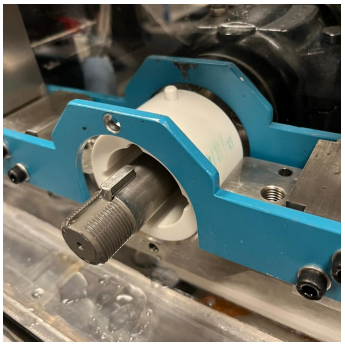

(a) Installed test bearing

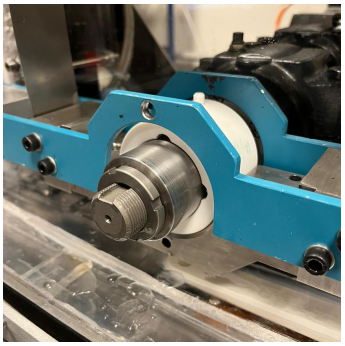

(b) Installed sleeve

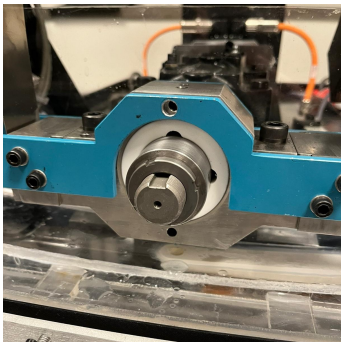

(c) Installed upper housing piece

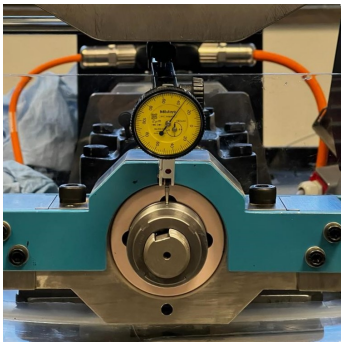

(d) Dial gauge reference

(e) Radial load digital readout

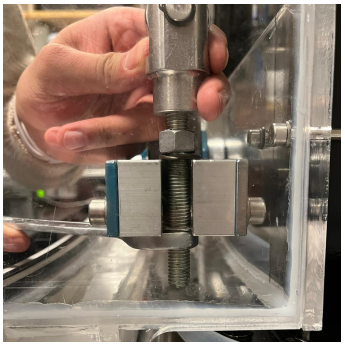

(f) Tighten nuts to apply preload

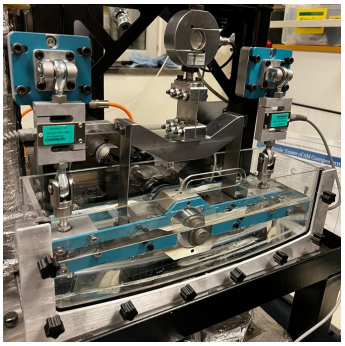

(g) Tank front panel installed

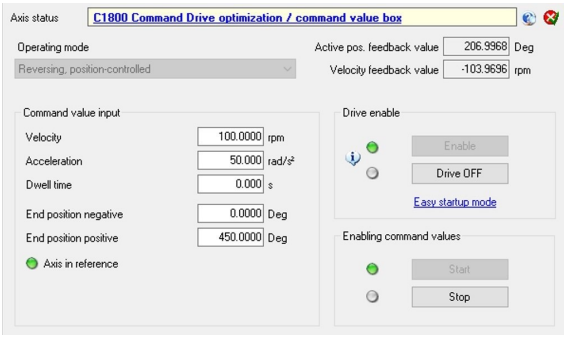

(h) Test parameters window

Fig. 5.9: Test Setup Procedure

Chapter 6

Results and Discussion

In this chapter, the results to verify the DAQ of the load cells are presented, the methodology used to test the sliding bearing is given and lastly the results are presented and discussed.

6.1 Load Cell Verification Tests

The load cells were directly connected to the National Instruments SCB-68A connection box. As there were doubts about the correct acquisition of the sensors, verification tests were performed.

To perform these tests, known weights were sequentially put on top of one load cell (compressing force). The results for the load cell used on the left and right sides of the test rig are shown in Fig. 6.1a and Fig. 6.1b, respectively.

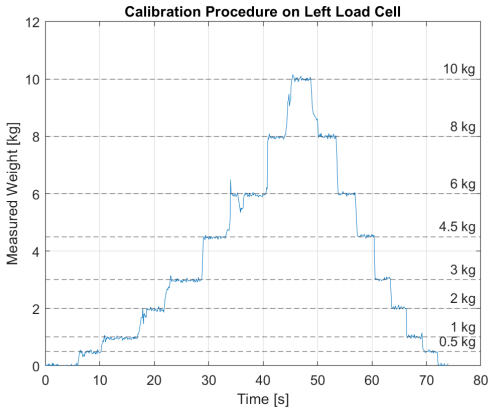

(a) Left load cell (SN: 325 643 33)

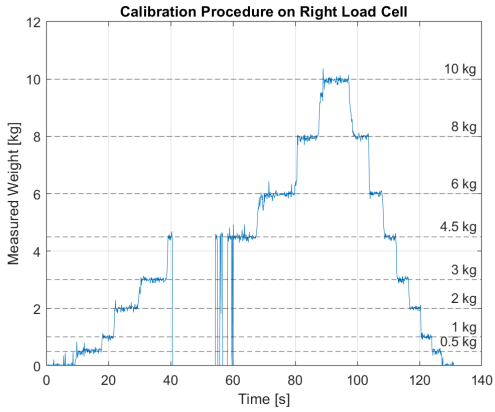

(b) Right load cell (SN: 325 643 54)

Fig. 6.1: Calibration results of the load cells used to measure the friction torque

For the zero to align correctly, a weight factor had to be added. For the left load cell (SN: 325 643 33 the factor was $0.2202kg$ and for the right load cell (SN: 325 643 54) the factor was $0.3108kg$. With these factors the measurements presented as very accurate. It must be said thought that this calibration tests were performed in compression, while the load cells are going to be used in tension.

The drop to zero in the middle of the calibration of the right load cell was due to a bad electrical contact between the connection box and the load cell wires. Once the bad contact was fixed, the test proceed.

For the load cell that only measures radial load, a similar calibration was used, but by looking at the numerical digital display connected to it. Here the procedure was a little different:

1. The bearing was mounted.
2. With an analogical dial gauge, the shaft deformation was measured while a radial load was applied. When the deformation was significant enough, the digital display was tared.
3. With the nut on the lever arm, the radial load was increased in steps of $30N$ until a load of $240N$ was achieved. A final additional load of $10N$ was applied to get a load of $250N$.

The results are presented in 6.2. As it is possible to see, the behavior is not the same as the other load cells. The steps of $30N$ cannot be depicted.

The configuration of the electrical box associated to this load cell needs further investigation. As the values of the display were considered correct, no changes were made. The radial load being recorded in the data acquisition software was not the most accurate but the initial number in the display was written down before each test for comparison.

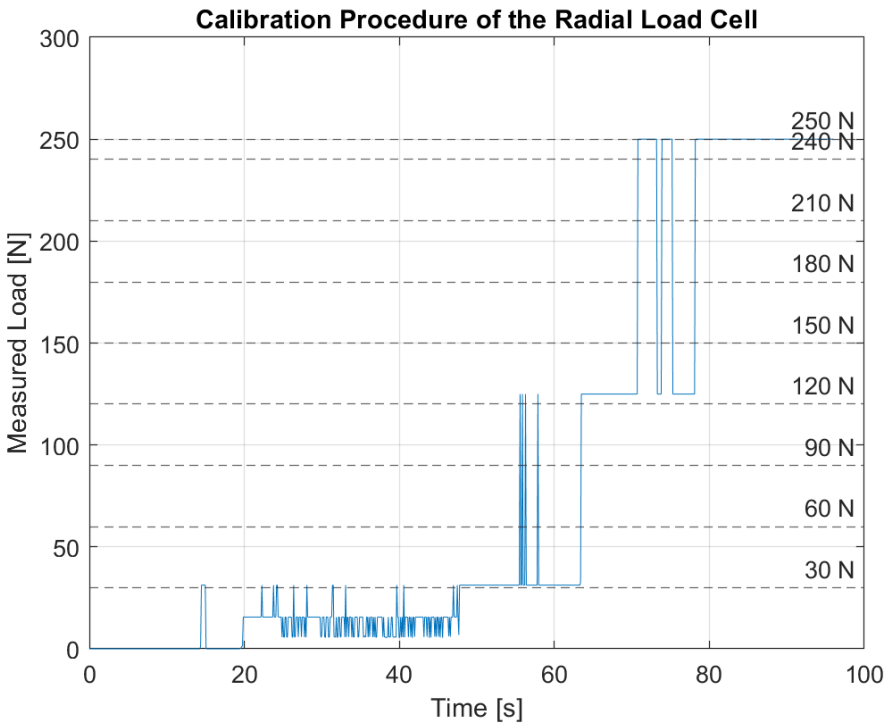

Fig. 6.2: Calibration results of the load cell used for measuring the applied radial load.

6.2 Methodology

After a description of how the machine works and is operated and after defining how the tests were performed, the results and discussion around them are performed.

The tidal turbine bearing test rig represents a critical platform to enhance the efficiency and reliability of tidal turbine technology. The machine is designed to assess the performance of reciprocating sliding bearings, integral to the power-take-off system of underwater tidal turbines.

As defined in the requirement list, the test rig needs to represent the characteristic use conditions of a tidal turbine sliding bearing. The requirements that describe the conditions are the following:

- The test rig shall offer the possibility to actuate the amplitude of oscillation of 1 Hz.
- The system shall be able to apply a contact pressure of 2 MPa.
- The test rig shall be able to apply a controllable amplitude (total range) of 45 degrees.

From the requirement's list it is possible to verify that the main parameters to vary are the speed profile (amplitude of the movement, acceleration and maximum speed), radial load applied to the bearing and duration of the test.

To prove that the requirements are fulfilled, two sets of conditions were set:

1. Test conditions set 1
    - Bearing: Vesconite Hilube
    - Radial Load: $750N$ (corresponding to $0.37MPa$)
    - Maximum Motor Velocity: $100rpm$ (corresponding to $20rpm$ in the shaft and a tangential velocity of $47.12mm/s$)
    - Acceleration: $50rad/s^2$
    - Dwell Time: $0s$
    - Amplitude of the movement (motor): $450deg$ (corresponding to $90deg$ in the shaft due to the gearbox)
2. Test conditions set 2
    - Bearing: Vesconite Hilube
    - Radial Load: $4600N$ (corresponding to $2.27MPa$)
    - Maximum Motor Velocity: $150rpm$ (corresponding to $30rpm$ in the shaft and a tangential velocity of $70.69mm/s$)
    - Acceleration: $70rad/s^2$
    - Dwell Time: $0s$
    - Amplitude of the movement (motor): $450deg$ (corresponding to $90deg$ in the shaft due to the gearbox)

A sample of the movement of both tests is presented in Fig. 6.3.

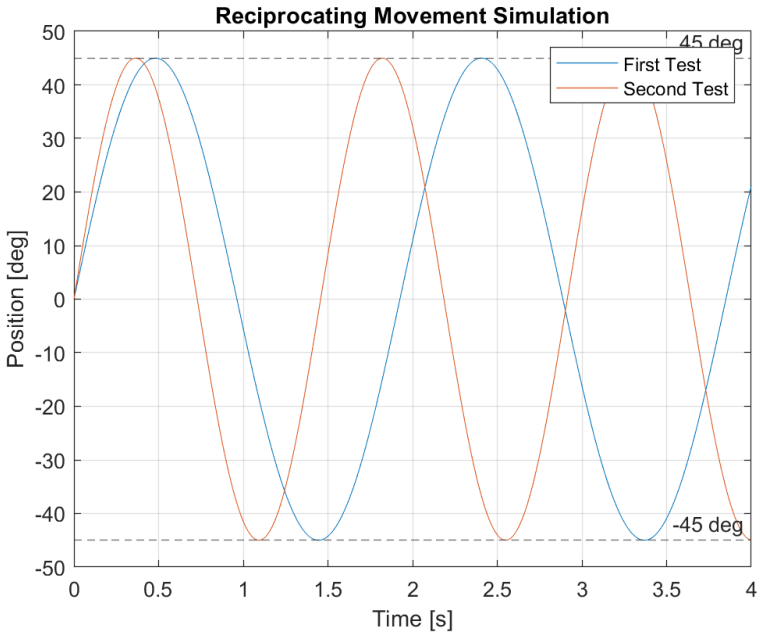

Fig. 6.3: Reciprocating movement profile of the tests

A third long test was attempted with a Vesconite Superlube but the radial load dropped considerably. The test was interrupted after 30 minutes. No pos-processing was performed on the data. The raw data will be provided in the course folder.

After the tests were performed, the bearings were removed and visually inspected. No further wear analysis was performed.

In the next section, the results of these two tests are going to be presented and discussed.

6.3 Results

6.3.1 Friction Measurement Results

After the tests were conducted, the data was saved and analyzed. As mentioned before in section 3.3.5, the first test was conducted with some parameters in the acquisition code that led to the data to not be synchronized. Therefore different pos-processing routines were used in the presented tests.

The factors mentioned in the calibration section were not used during pos-processing.

The first test lasted roughly 60 minutes while the second test lasted roughly 100 minutes.

To get the torque of the first test, some assumptions had to be layed down. Firstly, the reciprocating torque is symmetric, so the difference between the maximum and minimum loads measured by a single load cell will correspond to the equivalent load measured by the absolute sum of the two load cells. Secondly, the torque is approximately repeatable between consecutive movements.

With this assumptions, the torque for the first test was calculated using the difference between the moving maximum and moving minimum of each load cell using a span of 10 s (approximately 5 full cycles). This will overestimate the torque. A sample of the load cell reading is given in Fig. 6.4 and the variation of the moving minimum and maximum is given in Fig. 6.5.

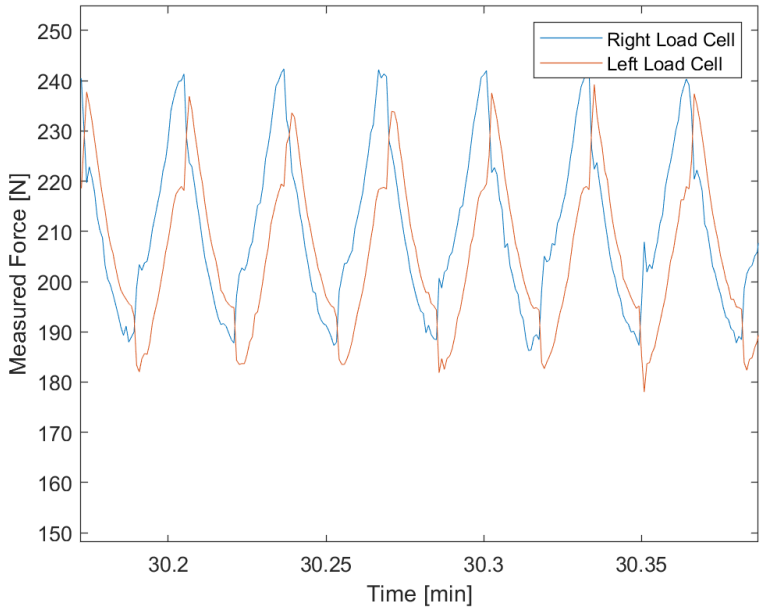

Fig. 6.4: Force sample of the test condition 1

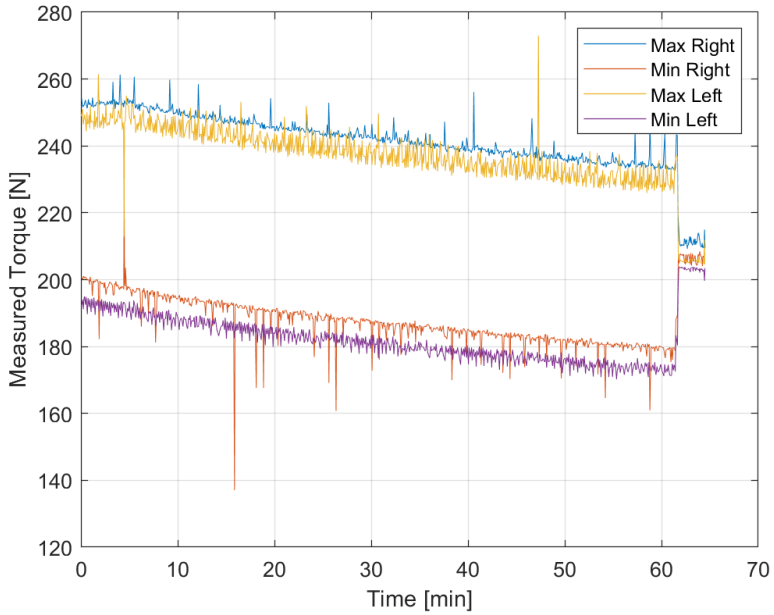

Fig. 6.5: Moving maximum and minimum results of the first test

It is possible to see from Fig. 6.4 that the torque never stabilizes, indicating that the maximum velocity is only achieved at the end of the movement, being constantly accelerating during the movement. As the encoder values were not being recorded it is difficult to validate this statement.

The variation of the friction torque and coefficient can be found in Fig. 6.6 and Fig. 6.7.

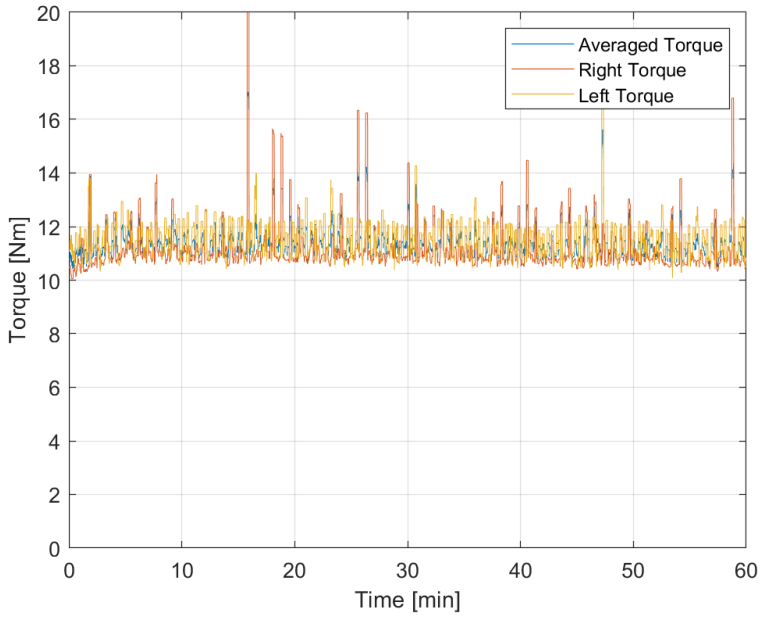

Fig. 6.6: Friction torque estimation from the data

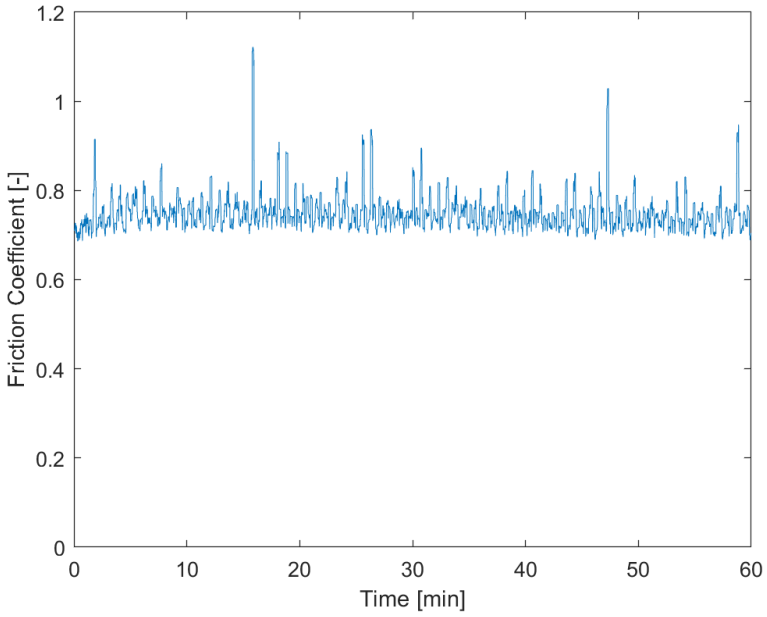

Fig. 6.7: Estimated friction coefficient

Again, the assumptions referred before point that this friction is too high.

For the second test, the data acquisition program was changed, so more trustworthy data was retrieved. A sample of the loads measured by the load cells are displayed in Fig. 6.8. The respective torque sample is presented in 6.9

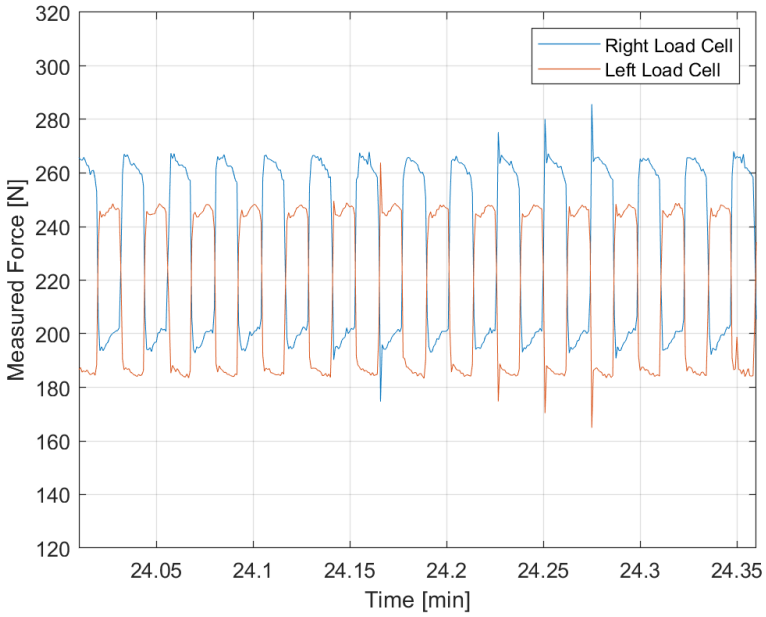

Fig. 6.8: Measured load sample.

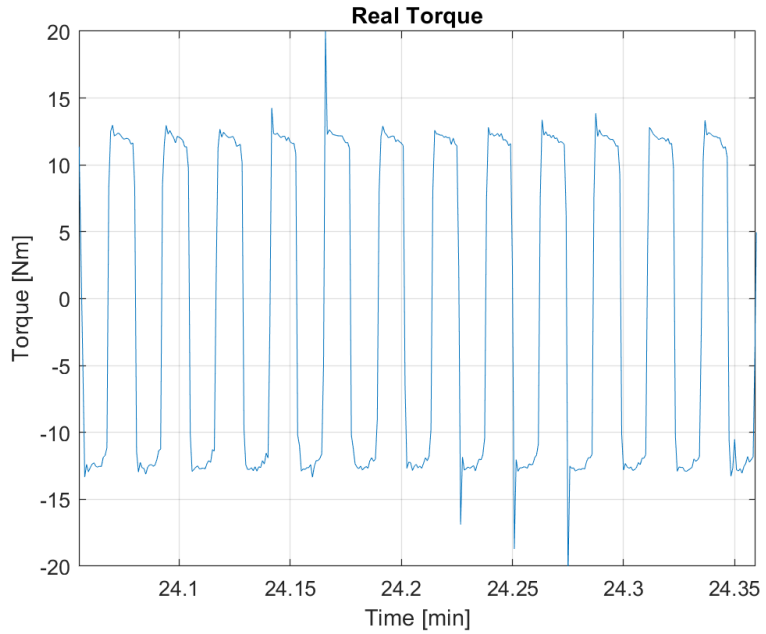

Fig. 6.9: Measured torque sample.

The radial load variation was determined by considering the moving minimum (of 4 cycles) of the moving maximum of the load cell reading of each cycle and subtracting to the moving maximum (of 4 cycles) of the moving minimum of each cycle. This way some instant peaks that can be seen in Fig. 6.8 were filtered. The radial load of each load cells were added as well as the initial load applied by the lever arm (it is known though that it also varies in time). The results are presented

in Fig. 6.10. It is possible to see that the radial load decreases along the test. The same phenomena was seen in the digital display connected to the load cell reading the radial load applied by the lever arm.

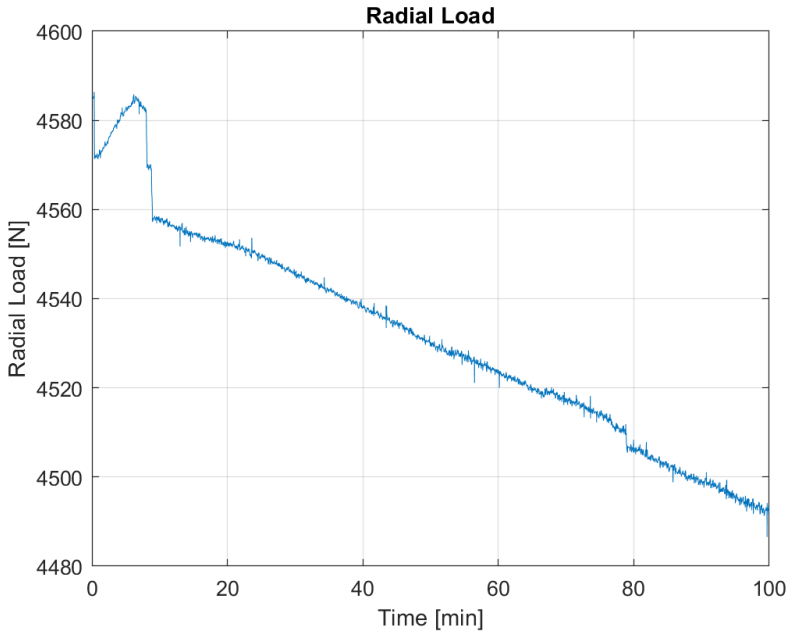

Fig. 6.10: Estimated radial Load variation along the test, only considering the side load cells.

From the information given in Fig.6.10 and Fig.6.9 it is possible to estimate the variation of the friction coefficient variation along the test. To do this a moving mean was applied to the absolute value of the friction torque and this value was divided by the radial load and radius of the bearing. The results are presented in Fig. 6.11.

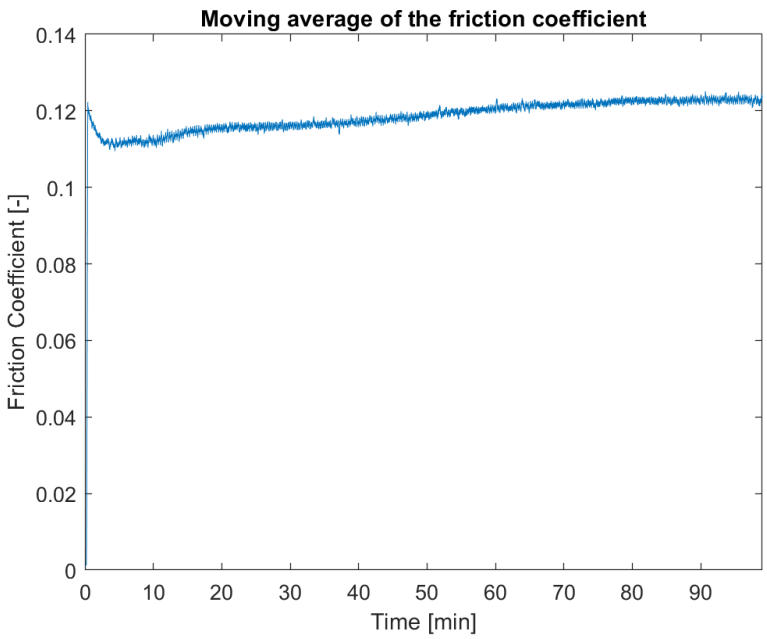

Fig. 6.11: Estimated friction coefficient variation along the test.

Data comparison

After presenting the data and the post-processing methods it is possible to conclude that a fair comparison between the two test results wouldn't be fair.

6.3.2 State of the Bearing after the tests

Photographs were taken to the bearing and sleeve surfaces after the test and are presented in Fig. 6.12 and 6.13.This surfaces were not evaluated in a profilometer.

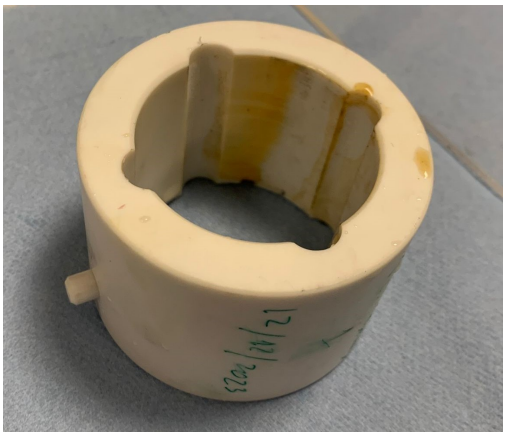

(a) Bearing

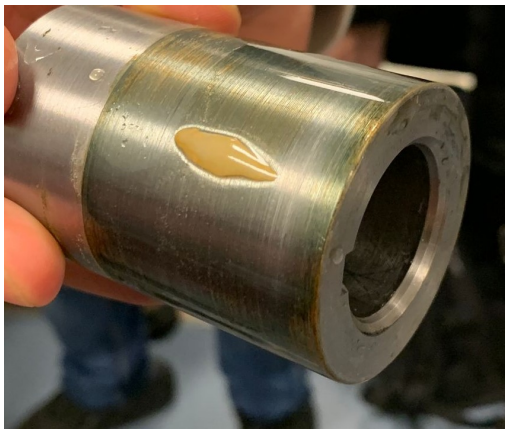

(b) Sleeve

Fig. 6.12: Bearing and sleeve after test 1.

Fig. 6.13: Bearing test 2.

6.4 Discussion

As referred in section 1.4, the requirements were set with the main stakeholders in the beginning of the project. During and after the project was developed, the requirements need to be verified.

The tests mentioned in the previous sections allowed the verification of some of the requirements.

The list of the requirements, priority attributed during the concept and design phase to each one of them and if they passed the verification are presented in Tab. 6.14

ID	Requirement	Priority	Fulfilled
1	The system shall replicate the operating conditions of the main shaft bearings of a tidal turbine	High	Yes
2	The test rig shall withstand the testing corrosive environment of seawater	High	Yes
3	The test rig shall offer the possibility to actuate the amplitude of oscillation of 1 Hz	High	Yes
4	The test rig shall fit sliding bearings	High	Yes
5	The test rig shall fit sealing rings	High	Yes
6	The test rig shall apply a variable radial load on the test sample applied at the beginning of the test	High	Yes
7	The test rig shall be able to apply a controllable amplitude (total range) of 45 degrees	High	Yes
8	The test rig shall be able to aquire friction torque data change with time	High	Yes
9	The test rig shall be able to aquire velocity data change with time	High	No
10	The test rig shall be able to aquire amplitude change with time	High	No
11	The test rig shall be able to aquire frequency change with time	High	No
12	The test rig shall be able to aquire radial load change with time	Medium	Yes
13	The test rig shall use the Scania journal bearing Test rig as a basis	High	Yes
14	The test rig shall be able to aquire vibration data of the module being tested	Medium	No
15	The test rig shall be able to aquire the temperature of the casing of the module being tested	Medium	No
16	The system shall be able to measure friction coefficient between 0 and 1 Nm per bearing with a precision of +/-1%	High	Yes
17	The system shall be able to apply a contact pressure of 2 MPa	High	Yes

Fig. 6.14: List of requirements, their priority and verification.

It is possible to see that out of 17 requirements set and revised by the stakeholders, 12 were verified. The main reasons behind not fulfilling the total number of requirements was the data acquisition system and sensors. Towards the manufacturing and testing phase it became clear that

the implementation of more sensors could lead to an allocation of resources that would not allow the fulfillment of other more important requirements.

In order to ensure that the system has the whole list of requirements, time and effort need to be put in the implementation of new electronics and update of the existing ones (computer and respective software).

Physical and mechanical requirements (requirements referring to loads, types of components, etc.) were all met and verified.

Chapter 7

Broader Impacts

This chapter discusses the broader implications of the final machine when considering its function, manufacturing, and distribution. Sections that do not apply to this project are noted with a brief description of why.

7.1 Engineering Ethics

The objective of this project was to build a research platform to study the tribology of tidal turbine bearings. This project employs all three fundamental principles in the codes of ethics for engineers:

1. The project uses our knowledge and skills to enhance human welfare. With the potential for discoveries into tidal energy converters, the technology can be developed and enhanced in quality for an improved transition to renewable energy.

2. The project is honest and impartial. It was made to the best of our abilities while being aware of the shortcomings discussed in our recommendations.

3. The project strives to increase the competence and prestige of the engineering profession. The project follows this, objecting to improve the prestige of the emerging tidal energy industry through greater competence in the tribology of components in saline water.

7.2 Societal and Global Impact

The main stakeholder of this project is the school, KTH, which will benefit from the ability to conduct tests on these new bearings. There is a potential for an unintended societal impact if the machine proves to help the understanding of tidal bearing performance in saline water. Catalyzing further investment and developments in renewable energy.

7.3 Environmental Impact

This project is beneficial to long-term sustainability for several reasons. Firstly this project revamped an existing testing rig. This reduced the amount of material needed to be manufactured and prevented production and shipping emissions. Also, this platform could lead to discoveries making tidal energy viable for commercial solutions. This has the potential to replace oil and coal energy production which is extremely detrimental to the environment.

7.4 Codes and Standards

As tidal energy is an emerging industry there are few technical codes or standards. Additionally, as this is not an industry product, such codes do not apply.

7.5 Economic factors

This section is not applicable as the machine is a one-off and not a commercial product.

Chapter 8

Conclusion

This year-long project has various outcomes. Firstly, the proof-of-concept test rig has been provided and can now be used by the *KTH Machine Design department*. Secondly, guidelines and recommendations have been given through that document to use the machine as efficiently as possible but also to support future work that could be performed on the same topic.

The first part of the project focused on understanding the context, the test rig requirements, the user's need but also the constraints linked to the development. With that information, work was done to produce a good design that would take into account all these considerations. Through this process, a lot of design iterations have been produced to end up with a design that would fit all our requirements and standards. These iterations were needed because new considerations have been discovered along the way as the needs and context were better understood. The next step was to find manufacturers and suppliers for the parts required, this part was especially under constraint as there were only a few weeks left before the project deadline. There was a need to come up with innovative techniques to deal with long delivery times or complicated manufacturing procedures. The last part was to mount the test rig and perform some tests to validate the concept presented.

While validating the test rig concept through manufacturing and testing, the future work needed was gathered. It aims at giving pieces of advice to make the rig more reliable, modular, and with a longer lifespan.

Another important outcome of the project and of the class is that a lot was learned by the group members. Not only about machine design but also about project planning, project methodology, and teamwork. The challenges faced throughout the project lifecycle served as valuable lessons and gave a better understanding of the importance of adaptability, problem-solving, and effective communication within a team setting.

The team now wishes that the machine and the information given will be useful to the *KTH Machine Design department* and that it can contribute, in the future, to a better understanding of tribological phenomenon.

Chapter 9

Future Work

The work done until then has delivered a test rig that is a proof of concept of the design ideas. Some modifications are still needed in order to transform the test rig into a reliable, high-life-span machine. The advised future work has been summarised in the following list:

- **Manufacture the new shaft in AISI 440**. The shaft should then be tempered at 316°C and a Hard Chrome Plating should be added. It is a good procedure to make the shaft resistant to very corrosive seawater. All the information on shaft dimensions and manufacturing requirements is provided.
- **Manufacture new sleeves** according to the studies that want to be conducted with the rig. The sleeve could be manufactured with AISI 316 to ensure a high lifespan of the component. The roughness specifications are provided by the sliding bearing manufacturer and depend on the test specifications.
- **Modifications to the tank.** The tank experienced some leakage during testing that was mostly attributed to the removable front panel. To mitigate this, new types of rubber should be evaluated as the current seal has a poor surface finish and a large force required to seal. Also, the structure should be reinforced with screws going through the aluminum sheet and the 2 acrylic sheets. This allows for higher pressure to be applied by the knob bolts onto the seal.
- **Determine the stiffness of the vertical sheets**. According to the multi-body simulations, the vertical sheets are not perturbing too much the measurements but their stiffness may have an impact on the final value. By measuring their stiffness, their influence can be evaluated and compensated in the post-process. It will allow for more precise measurements.
- **Improve electrical implementation**. The load cells have been connected directly to the NI DAQ box. The cable organization can be improved. Furthermore, the radial load cell implementation should be revised in order to have better readings and data acquisition in LabView. Additionally, the excitation of the load cells is being performed using an external power source. Power from the electrical box can be sued to excite the load cells. The new load cells make use of 6 wires (2 for excitation, 2 for signal and 2 for sense); currently the sense wires are not being used properly, so a new acquisition method can be thought in order to include this capability.
- **Improve LabView program**. The LabView file provided with the test rig only has a proof of concept objective. It could be improved to feature more data or display it differently in order to be more convenient for the users. Integrating the

- **Update computer**. During testing and during the development of the programs, it was noted that the computer used to control the motor and save the data is slow. Updating the computer to one more recent would increase the productivity of the test. Furthermore, updating the used softwares to more recent versions would facilitate future implementations. One case of it is connecting the motor encoder to LabView. Currently, the encoder data is not being recorded and the main reason can be attributed to the version of LabView (2018). Newer versions accept more recent and complete add-ons developed by Bosch Rexroth that enable a smoother implementation of this feature.

- **Add a temperature measurement**. Measuring the temperature inside the load cell can be interesting for some applications. Therefore, a temperature probe or thermocouple that could function in seawater could be added to the design. Currently, the design already includes a tap hole to hold a thermocouple coupling. The National Instruments connection box can be used to acquire its signal.

- **Make the rig modular to test other types of components**. The concept and the rig presented are used to test sliding bearings but the test rig could be modified to test other components such as another type of bearings, seals, or gears under seawater or other liquids. The actual concept should be kept but the connection elements would have to be modified. This improvement should be done after the other steps and could lead to another machine design project.

- **Repeat the testing of the bearings and test new bearings**. As shown in the Results chapter, it is advisable to re-do the tests in a more structured way, using better informed conditions (speed, acceleration, frequency, loading, etc.). It is also advisable to study the wear patterns in the inner surface of the bearing in order to predict the life of the system.

Bibliography

[1] T. S. Marcus Gralde Axel Lison Almkvist and S. Wassie, *Journal bearing test rig report*, 2013.

[2] H. S. Han and K. H. Lee, "Experimental verification of the mechanism on stick-slip nonlinear friction induced vibration and its evaluation method in water-lubricated stern tube bearing," *Ocean Engineering*, vol. 182, pp. 147–161, 2019.

[3] M. Ali, T. Ravens, T. Petersen, A. Bromaghin, and S. Jenson, "Impact of sediments on wear performance of critical sliding components of hydrokinetic devices," *Renewable Energy*, vol. 80, pp. 498–507, 2015.

[4] A. Barszczewska, "Experimental research on insufficient water lubrication of marine stern tube journal bearing with elastic polymer bush," *Polish Maritime Research*, vol. 27, no. 4, pp. 91–102, 2020.

[5] H. Allmaier, C. Priestner, C. Six, H. Priebsch, C. Forstner, and F. Novotny-Farkas, "Predicting friction reliably and accurately in journal bearings—a systematic validation of simulation results with experimental measurements," *Tribology International*, vol. 44, no. 10, pp. 1151–1160, 2011.

[6] D. E. Sander, H. Allmaier, H. H. Priebsch, M. Witt, and A. Skiadas, "Simulation of journal bearing friction in severe mixed lubrication–validation and effect of surface smoothing due to running-in," *Tribology international*, vol. 96, pp. 173–183, 2016.

[7] D. E. Sander, H. Allmaier, H.-H. Priebsch, *et al.*, "Impact of high pressure and shear thinning on journal bearing friction," *Tribology international*, vol. 81, pp. 29–37, 2015.

[8] Z. Xie and W. Zhu, "Theoretical and experimental exploration on the micro asperity contact load ratios and lubrication regimes transition for water-lubricated stern tube bearing," *Tribology International*, vol. 164, p. 107 105, 2021.

[9] W. Litwin, M. Wasilczuk, M. Wodtke, and A. Olszewski, "The influence of polymer bearing material and lubricating grooves layout on wear of journal bearings lubricated with contaminated water," *Tribology International*, vol. 179, p. 108 159, 2023.

[10] [Online]. Available: `https://www.ringfeder.com/products/locking-assemblies/rfn-7012/`.

[11] D. 1. /. M. A. Budden, 2011. [Online]. Available: `https://www.cgtk.co.uk/metalwork/data/morse`.

[12] A. Van Beek, "Advanced engineering design: Lifetime performance and reliability (vol. 1)," 2006.

[13] A. Van Beek, *Tribology abc*. [Online]. Available: `https://www.tribology-abc.com/`.

[14] *Steel international_2023*, Nov. 2023. [Online]. Available: `https://steeltube.co.in/tag/316-stainless-steel-hardness-hrc/`.

[15] C. Tower and C. Foothill Ranch, "Chrome plating: A guide for selecting the type of chrome plating for use in contact with bal seal® spring-energized seals in rotary and reciprocating service," 2016.

[16] V. S. Helbert, M. Dhondt, R. Homette, S. A. Chirani, and S. Calloch, "Effect of mechanical preloadings on corrosion resistance of chromium-electroplated steel rods in marine environment," *Materials Research Express*, vol. 5, no. 3, p. 036 522, 2018.

[17] H. Dresig and F. Holzweißig, *Dynamics of machinery: theory and applications*. Springer Science & Business Media, 2010.

[18] *Trelleborg rotary seals catalogue 2023*, 2023.

Appendix A

Comparison of Shaft Material

Material Family	Minimum Price [SEK/Kg]	Young's Modulus [GPa]	Yield Strength [MPa]***	Fatigue Strength at 10^7 cycles [MPa]***	Hardness [HRC]	Galling resistance **	Stress corrosion cracking **	Resistance to Sea Water **
AISI 316L	Stainless Steel	55.5	190	170	256	1-19	Acceptable	Slighlty Susceptable	Good
AISI 440C, annealed	Stainless Steel	15.6	190	405	341	13-26	Acceptable	Slighlty Susceptable	Restricted
AISI 440C, tempered at 316°C	Stainless Steel	15.6	190	1710	638	53-60	Excellent	Susceptible	Restricted
AISI 2205	Duplex Stainless Steel	82.4	195	460	261	22-31	Limited Use	Not susceptible	Good
INCOLOY 945X	Nickel-Iron-Chromium Alloy	310.0	195	914	525	39-41	Acceptable	Not susceptible	Excellent
S275JR	None alloyed structural steel	11.6	205	275	199	<1	Acceptable	Slighlty Susceptable	N.S.***

* Minimum value given by Granta Edupack Level 3
** Classification given in Granta Edupack Level 3
*** Not specified by the program given that it is not a Stainless Steel

Appendix B

Granta Edupack material property description

B.1 B1 - Resistance to Sea Water

Qualitative category	*Explanation*
Poor	Poor resistance, uniform corrosion could occur in the environment
Restricted	Material should be considered for this environment for low exposure times only
Moderate	Material could be used in the environment but with restrictions (i.e. low temperatures, or low exposure time)
Good	Material commonly used in this environment, but might have a warning for some specific cases (i.e. high temperatures)
Excellent	Material commonly used in this environment without restriction

B.2 B2 - Stress corrosion cracking

The resistance of the material to stress corrosion cracking (SCC). Crack growth is caused by the combined effects of stress and chemical attack.

As all materials presents are Carbon Steels, the ambient in which they are being categorized is Chloride

Materials are categorized qualitatively on the following four-point scale:

- Highly susceptible
- Susceptible
- Slightly susceptible
- Not susceptible

Four factors are required for SCC to occur:

- The part must be stressed (applied force or residual stress).

- The environment must be aggressive.
- The metal must be susceptible to the environment.
- The duration of service must be sufficient to permit the initiation and growth of cracks.

B.3 B3 - Galling resistance

Qualitative category	*Explanation*
Excellent	The material is suitable for applications or mating with materials in which galling is a major issue and will only gall in exceptional circumstances.
Acceptable	The material is suitable for applications which require galling resistance without additional treatments, although have a tendency to gall in some circumstances.
Limited use	The material is suitable for applications which require galling resistance subject to careful lubrication, additional treatments or in specific circumstances detailed in notes.
Unacceptable	The material is not used for any applications which require galling resistance and are difficult to process due to this type of wear.